Figure 2. **SC thickness measured by conventional histological methods and filaggrin immunostaining.** Note remarkably increased SC thickness in filaggrin-related AD (a) due to an increased number of cornified cell layers. Immunohistochemical staining with anti-filaggrin monoclonal antibody against an epitope conserved in all filaggrin repeat peptides revealed a marked reduction of filaggrin staining in the epidermis of filaggrin-related AD (e) and IV without concomitant AD (g). (a–d) Hematoxylin and eosin staining; (e–h) filaggrin immunostaining. (a, e) Patient number 3 with compound heterozygous *FLG* mutations, c.3321delA, and p.Ser2554X (filaggrin-related AD); (b, f) patient number 21 without any *FLG* mutation (non-filaggrin AD); (c, g) patient number 27, IV without concomitant AD, harboring heterozygous *FLG* mutation p.Ser2554X; (d, h) normal control. Bars, 25 μm.

scores for any antigen between filaggrin-related AD and non-filaggrin AD.

Neither EOS, total serum IgE nor serum LDH showed any apparent association with the OSCORAD in either filaggrin-related AD or non-filaggrin AD by Wilcoxon rank sum test. Although no significant correlation was obtained between EOS, total serum IgE, LDH, and the OSCORAD in either filaggrin-related AD or in non-filaggrin AD by simple regression test, the OSCORAD and specific IgE for several allergens in filaggrin-related AD revealed a significant correlation coefficient, such as between OSCORAD and IgE for house dust (correlation coefficient $r = 0.66$, $P < 0.05$) in filaggrin-related AD, between the OSCORAD and IgE for mite allergen (correlation coefficient $r = 0.53$, $P < 0.05$) in filaggrin-related AD, and between the OSCOR-AD and IgE for cat dander (correlation coefficient $r = 0.64$, $P < 0.05$) in filaggrin-related AD. IgE for the other allergens in filaggrin-related AD did not show any correlation with the OSCORAD. IgE MAST scores for none of the allergens exhibited any correlations with the OSCORAD in non-filaggrin AD.

DISCUSSION

Atopic dermatitis is thought to comprise a group of patients with heterogeneous pathogenic factors. For a long time, abnormalities in the immune system have been highlighted as causative factors underlying AD. Recently, *FLG* mutations

were found to be an important predisposing factor for AD and epidermal barrier defects have been attracting attention as an important pathomechanisms leading to AD.

The epidermal barrier function, in ichthyosis patients measured by SC hydration, thickness, and TEWL are known to be associated with the severity of the disease (Tomita *et al.*, 2005). Additionally, in AD patients, TEWL was reported to be increased, although controversy still remains as to whether the defective barrier function in AD patients is a primary cause of AD or a secondary consequence following dermatitis (Leung, 2000). Several studies have proven that there is a close correlation between clinical severity assessed using the SCORAD and skin barrier dysfunction in AD patients (Chamlin *et al.*, 2002; Sugarman *et al.*, 2003).

Stratum corneum hydration was marginally lower in filaggrin-related AD compared to non-filaggrin AD, although no statistical significance was obtained between our two AD groups. In contrast, TEWL was higher in non-filaggrin AD compared to in filaggrin-related AD. Low SC hydration in filaggrin-related AD might be indirectly related to barrier defects, but could primarily be related to a deficiency of water-binding filaggrin breakdown products (natural moisturizing factor) within the SC of filaggrin-related AD patients.

From the results of the present study, SC thickness was significantly thicker in filaggrin-related AD than in non-filaggrin AD. In contrast, the TEWL increase observed in
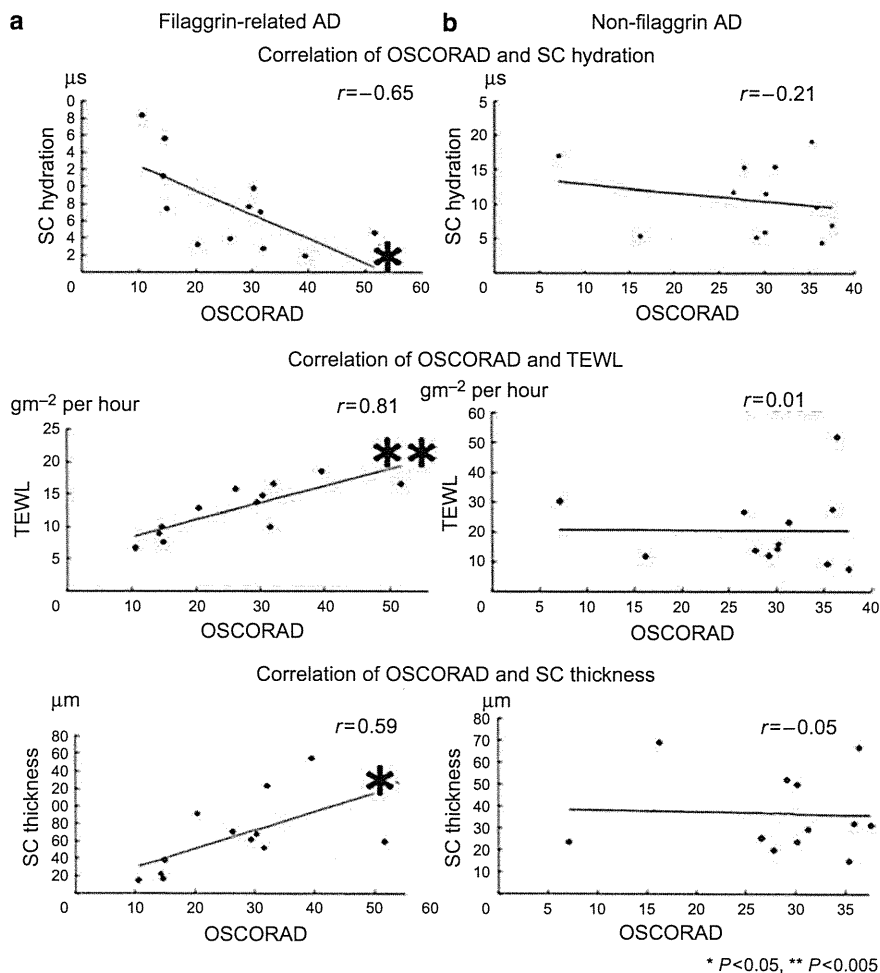
a Filaggrin-related AD   **b** Non-filaggrin AD

Correlation of OSCORAD and SC hydration

Correlation of OSCORAD and TEWL

Correlation of OSCORAD and SC thickness

$* P<0.05, ** P<0.005$

Figure 3. Correlation of clinical severity (OSCORAD) and SC hydration (average values of the three regions, μs), OSCORAD and TEWL (average values of the three regions, $g\,m^{-2}$ per hour), and OSCORAD and SC thickness (average values of the three regions, μm). (a) Filaggrin-related AD. A significant correlation was shown between OSCORAD and each parameter. Data with P-values $*P<0.05$ were evaluated as significant and $**P<0.005$ were evaluated as highly significant. (b) Non-filaggrin AD. No statistically significant correlation was shown between OSCORAD and any parameter.

non-filaggrin AD was significantly greater than that in filaggrin-related AD. It appears interesting that there seems to be a clear difference in barrier formation (SC thickness) and function (TEWL) between the two groups. In total, 4 patients out of 12 in filaggrin-related AD exhibited concomitant IV, although none of non-filaggrin AD patients had concomitant IV. Thus, we cannot exclude the possibility that remarkable SC thickness in filaggrin-related AD is related to the IV characteristics of patients, though SC was generally thinner in IV patients without AD in the present study. In addition, in our study, a negative correlation between the clinical AD severity (OSCORAD) and SC hydration and a positive correlation between the OSCORAD and TEWL were confirmed only in filaggrin-related AD. There was no significant correlation between the OSCORAD and SC hydration and between the OSCORAD and TEWL in non-filaggrin AD. However, according to a previous report studying French AD patients (Hubiche *et al.*, 2007), no significant difference was observed in the level of barrier function defects between

filaggrin-related AD and non-filaggrin AD. It should be noted that in the previous study (Hubiche *et al.*, 2007), that the AD cohort was screened only for the two common filaggrin mutations, p.R501X, and c.2282del4 and was not screened for the many newly identified European filaggrin mutations, some of which are also prevalent in European populations (Sandilands *et al.*, 2007).

The OSCORAD scoring in the present study showed slight skewing between the two AD groups. Filaggrin-related AD seemed in general to have a relatively low OSCORAD score. This fact could have affected the interpretation of the other data. The effect of omitting treatments for 24 hours might also make non-filaggrin AD patient's disease worse than that of filaggrin-related AD patients. Thus, we checked this skewing using the Wilcoxon rank sum test and box-whisker plots, whereby the skewing was in fact revealed to be nonsignificant (Figure S1). No clinically relevant differences were seen between filaggrin-related AD and non-filaggrin AD in the present study.

—78—

From our results, increased SC thickness, TEWL, and reduced SC hydration are thought to be good indicators to evaluate the severity of filaggrin-related AD. Furthermore, in filaggrin-related AD, increased SC thickness and TEWL and reduced SC hydration might be useful to predict clinical course of the patients. In addition, given the strong correlations between the AD severity score (OSCORAD) and all the three parameters of skin barrier (TEWL, SC hydration, and thickness) obtained only in filaggrin-related AD, we are able to speculate that epidermal barrier defects may be one of the primary abnormalities in filaggrin-related AD.

Only in filaggrin-related AD, significant positive correlations were confirmed between the OSCORAD and IgE for house dust, between the OSCORAD and IgE for mite allergen, and between the OSCORAD and IgE for cat dander. There was no significant correlation between the OSCORAD and allergen-specific IgE in non-filaggrin AD. These results indicated the possibility of percutaneous sensitization for the allergens due to skin barrier defects in filaggrin-related AD. Mechanisms by which barrier defects due to *FLG* mutations contribute to the overall clinical end points of AD have yet to be completely clarified. Profilaggrin/filaggrin is crucial for maintaining the epidermal barrier function (Hudson, 2006). *FLG* mutations result in complete or incomplete loss of profilaggrin/filaggrin peptides and seem to be important in facilitation of allergic sensitization in AD patients. Defective epidermal barrier function provides easy access of allergens, antigens, and irritants through the epidermis, leading to stimulation of active T cells that contribute to more inflammation of the skin (Leung *et al.*, 1995).

We examined the histopathological features of three patients, one filaggrin-related AD, one non-filaggrin AD, and one IV without concomitant AD. Our results demonstrate that SC thickness measured in conventional histological slides correlated well to SC thickness as measured by a corneometer. Concordance of SC thickness measured by a corneometer and that measured by conventional histological methods was previously reported in ichthyosis patients (Tomita *et al.*, 2005). Thus, we feel that SC thickness measured by a corneometer without any further invasive procedures may be a useful and reliable parameter of hyperkeratosis. From histopathological observations, the thickening of SC in filaggrin-related AD (patient 3) appeared to be due to an increased number of cornified cell layers in SC. This observation suggests that hyperkeratosis in filaggrin-related AD might be caused by reduced desquamation of cornified cells, but not by diminished compaction of the corneocytes in the SC. These observations further emphasize the close pathophysiological relationship between ichthyosis vulgaris and filaggrin-related AD.

In our study, AD patients showing aggravation in summer were restricted to the AD group of the patients without *FLG* mutations, although the number of patients included in the present study was limited. Overexposure to sweat antigens was suggested to be an accelerating factor for AD eczema (Tanaka *et al.*, 2006). AD patients with summer aggravation

might have other predisposing factors including sweat antigen exposure, but not epidermal barrier defects. Further study with a larger number of patients is needed to verify this hypothesis.

Our results showed remarkable barrier dysfunction (increased TEWL) in AD patients who did not have any *FLG* mutations. Jakasa *et al.* (2007) reported altered penetration of polyethylene glycols into uninvolved AD patient skin. There are likely a variety of mechanisms that modulate barrier integrity, other than the profilaggrin/filaggrin system, although it should be noted that there may be other filaggrin mutations still remain undetected in the Japanese population. Other structural molecules may also contribute to skin barrier formation by as yet unknown mechanisms.

MATERIALS AND METHODS
Patients
We selected 24 patients with AD according to criteria proposed by Hannifin and Rajka (1980), 14 males and 10 females, with a mean age of 21.36 years (range, 6–33 years). Twelve patients harbored *FLG* mutations (filaggrin-related AD) and the other twelve patients had no apparent *FLG* mutation (non-filaggrin AD). They were all treated by topical steroid ointment ranged from moderate to very strong, topical tacrolimus, moisturizer (heparinoid), or oral anti-histamines. We interviewed patients about disease duration of AD, presence or absence of family history of AD, and other atopic disorders including asthma or allergic rhinitis, and seasonal difference in AD severity. Patient numbers 3, 4, 10, and 11 had features of concomitant IV including hyperlinearity in the palms and scales on the lower legs. Patient numbers 1, 2, 5, 6, 7, 8, 9, 12, and 13–24 had dry skin, but no apparent concomitant IV features. In addition, three typical IV patients without concomitant AD harboring *FLG* mutations were included in the present study.

Age-matched healthy volunteers were included in the present study as controls. The control group consisted of 12 healthy individuals aged 6–30 years (eight male and four female) without any past or present skin disease.

The present study was approved by the Institutional Ethical Committee of Hokkaido University Graduate School of Medicine. This study was conducted according to all the Declaration of Helsinki Principles. Participants or their legal guardians gave their written informed consent.

Filaggrin genotyping
FLG mutation analysis was performed in patients and their family members. Briefly, genomic DNA isolated from peripheral blood was subjected to PCR amplification, followed by direct automated sequencing using ABI PRISM 3100 or 3730 genetic analyzers (Applied Biosystems, Foster City, CA). Mutations p.Ser2554X, p.Ser2889X, and p.Ser3296X were screened using restriction enzyme digestion of PCR products (Nomura *et al.*, 2007, 2008). Mutation c.3321del was screened by fluorescent PCR (Nomura *et al.*, 2007). Primers and PCR conditions were as described previously (Nomura *et al.*, 2007, 2008).

Disease severity
The SCORAD (severity scoring of AD, score range 0–103; European Task Force on Atopic Dermatitis, 1993) utilizes the rule of nines with

six clinical features of AD disease intensity: erythema/darkening, edema/papulation, oozing/crust, excoriations, lichenification/prurigo, and dryness. Dryness was evaluated on noninflamed skin. The other features were assessed on a representative area for a given intensity item, also on a scale of 0–3. To measure AD clinical severity, we employed the objective SCORAD (OSCORAD; score range 0–83; Holm *et al.*, 2006). In the OSCORAD, which is often used in clinical trials, two subjective symptoms (itch and sleep loss) were excluded from the conventional SCORAD.

Measurement of stratum corneum hydration, TEWL, and stratum corneum thickness

Measurements were performed under standardized conditions, that is, at a room temperature of 22–25 °C and a humidity level of 40–55%. Before the measurements, patients were given time to adapt to room conditions without covering the measurement sites with clothes. All the measurements were performed by one investigator (INH). Almost all patients were taking anti-histamines, and treated by topical steroids, topical immunosuppressants, emollients (heparinoid), which were all kept maintained. However, from 2100 hours on the day before the investigation, nothing was applied to the skin to be examined. To exclude the bias of different dermatitis severities in the examination sites, three body sites, clinically normal areas in the extensor and flexor aspects of the forearm and on the back, were selected for examination. All measured values were expressed as the median of three recordings to avoid measuring inaccuracies. SC hydration was measured as (low-frequency susceptance) × (square root of electrode distance)/(square root of low frequency conductance) by using noninvasive methods (Yamamoto, 1994) with a Corneometer ASA-M2 (ASAHI BIOMED, Yokohama, Japan). ASA-M2 evaluated conductance of two different electric currents with low frequency and high frequency. The low-frequency current was limited to the superficial SC and the high-frequency current penetrated the highly moist region immediately below the SC. Thus, SC thickness was calculated from low-frequency susceptance and high-frequency admittance by the corneometer as (square root of low-frequency susceptance)/(high-frequency admittance; Yamamoto, 1994). TEWL was measured using Evaporimeter AS-TW1 (ASAHI BIOMED, Yokohama, Japan). AS-TW1 utilizes the ventilated chamber method of measuring TEWL. Its hygrometer measures the humidity of incoming air and of outgoing air that has passed over the test area of skin, and TEWL is calculated from the difference. TEWL measurements were done on the extensor and flexor sides of the forearm that were observed clinically normal. All the measurements were performed three times for each skin spot.

Immunohistochemical staining

Immunoperoxidase staining of paraffin-embedded sections was performed using the ChemMate Peroxidase/DAB system (Dako Cytomation, Hamburg, Germany). Mouse monoclonal antibody 15C10 (Novocastra, Newcastle, UK) was used to detect the human filaggrin repeat unit. Antigen retrieval was performed by heating sections under pressure for 10 to 15 minutes in $10 \, \text{nmol l}^{-1}$ citrate buffer, pH 6.0.

Laboratory tests

Peripheral blood EOS count (number × 100 per µl; normal 40–440), serum LDH ($IU \, l^{-1}$; normal 119–229), total serum IgE ($IU \, ml^{-1}$;

normal 0.0–400.0), and allergen-specific IgE (SRL Inc., Tokyo, Japan) were measured. Allergen-specific IgE were estimated by fluoroenzyme immunoassays for house dust, mite allergen, grass pollen (*Tancy*), cedar pollen, fungal allergen (*Candida*), animal dander, and foods. Concerning to the sensitivity for detection of specific IgE, 100 lumicount and values greater than or equal to 100 lumicount were considered positive (+).

Statistical analysis

Statistical analysis was performed using Excel 2000 (Microsoft, Redmond, WA) with the add-in software Statcel 2 (OMS, Saitama, Japan) and JMP 6.0.3 (SAS Institute, Tokyo, Japan). Wilcoxon rank sum and Turkey–Kramer's honestly significant difference tests were used to compare the continuous variables between the group of total AD patients and normal controls, and between filaggrin-related AD and non-filaggrin AD. Data with *P*-values less than 0.05 were evaluated as significant. We interpreted *P*-values less than 0.01 as highly significant.

Simple regression analyses were also used to identify significant associations of SC hydration, thickness, or TEWL to OSCORAD. Data with *P*-values less than 0.05 were evaluated as significant. We interpreted *P*-values less than 0.005 as highly significant. Wilcoxon rank sum test and simple regression analyses were performed to assess the association or correlation between different biological markers including IgE, LDH, EOS, and the OSCORAD.

SUPPLEMENTARY MATERIAL

Table S1. Clinical information on the patients and FLG mutations.

Table S2. Patients' clinical severity (OSCORAD), SC hydration, TEWL, and SC thickness.

Figure S1. Box-whisker plots of OSCORAD in the two AD groups. Wilcoxon rank sum test and box-whisker plots revealed no significant difference in OSCORAD scores between filaggrin-related AD and non-filaggrin AD.

REFERENCES

Aalto-Korte K (1995) Improvement of skin barrier function during treatment of atopic dermatitis. *J Am Acad Dermatol* 33:969–72

Chamlin SL, Kao J, Frieden IJ, Sheu MY, Fowler AJ, Fluhr JW *et al.* (2002) Ceramide-dominant barrier repair lipids alleviate childhood atopic dermatitis: changes in barrier function provide a sensitive indicator of disease activity. *J Am Acad Dermatol* 47:198–208

European Task Force on Atopic Dermatitis (1993) Severity scoring of atopic dermatitis: the SCORAD index. *Dermatology* 186:23–31

Hannifin JM, Rajka G (1980) Diagnostic features of atopic dermatitis. *Acta Derm Venereol* 92:44–7

Hata M, Tokura Y, Takigawa M, Sato M, Shioya Y, Fujikura Y *et al.* (2002) Assessment of epidermal barrier function by photoacoustic spectrometry

—80—

in relation to its importance in the pathogenesis of atopic dermatitis. *Lab Invest* 82:1451–61

Holm EA, Wulf HC, Thomassen L, Jemec GB (2006) Instrumental assessment of atopic eczema: validation of transepidermal water loss, stratum corneum hydration, erythema, scaling, and edema. *J Am Acad Dermatol* 55:772–80

Hubiche T, Ged C, Benard A, Leaute-Labreze C, McElreavey K, de Verneuil H *et al.* (2007) Analysis of SPINK 5, KLK 7 and FLG Genotypes in a French Atopic Dermatitis Cohort. *Acta Derm Venereol* 87:499–505

Hudson TJ (2006) Skin barrier function and allergic risk. *Nat Genet* 38:399–400

Irvine AD, McLean WHI (2006) Breaking the (un) sound barrier: filaggrin is a major gene for atopic dermatitis. *J Invest Dermatol* 126:1200–2

Jakasa I, de Jongh CM, Verberk MM, Bos JD, Kezic S (2006) Percutaneous penetration of sodium lauryl sulphate is increased in uninvolved skin of patients with atopic dermatitis compared with control subjects. *Br J Dermatol* 155:104–9

Jakasa I, Verberk MM, Esposito M, Bos JD, Kezic S (2007) Altered penetration of polyethylene glycols into uninvolved skin of atopic dermatitis patients. *J Invest Dermatol* 127:129–34

Leung DY (2000) Atopic dermatitis: new insights and opportunities for therapeutic intervention. *J Allergy Clin Immunol* 105:860–76

Leung DY, Travers JB, Norris DA (1995) The role of superantigens in skin disease. *J Invest Dermatol* 105:37S–42S

Nomura T, Sandilands A, Akiyama M, Liao H, Evans AT, Sakai K *et al.* (2007) Unique mutations in the filaggrin gene in Japanese patients with ichthyosis vulgaris and atopic dermatitis. *J Allergy Clin Immunol* 119:434–40

Nomura T, Akiyama M, Sandilands A, Nemoto-Hasebe I, Sakai K, Nagasaki A *et al.* (2008) Specific filaggrin mutations cause ichthyosis vulgaris and are significantly associated with atopic dermatitis in Japan. *J Invest Dermatol* 128:1436–41

Palmer CNA, Irvine AD, Terron-Kwiatkowski A, Zhao Y, Liao H, Lee SP *et al.* (2006) Common loss-of-function variants of the epidermal barrier protein filaggrin are a major predisposing factor for atopic dermatitis. *Nat Genet* 38:441–6

Rawlings AV, Harding CR (2004) Moisturization and skin barrier function. *Dermatol Ther* 17:43–8

Roll A, Cozzio A, Fischer B, Schmid-Grendelmeier P (2004) Microbial colonization and atopic dermatitis. *Curr Opin Allergy Clin Immunol* 4:373–8

Sandilands A, Terron-Kwiatkowski A, Hull PR, O'Regan GM, Clayton TH, Watson RM *et al.* (2007) Comprehensive analysis of the gene encoding filaggrin uncovers prevalent and rare mutations in ichthyosis vulgaris and atopic eczema. *Nat Genet* 39:650–4

Smith FJD, Irvine AD, Terron-Kwiatkowski A, Sandilands A, Campbell LE, Zhao Y *et al.* (2006) Loss-of-function mutations in the gene encoding filaggrin cause ichthyosis vulgaris. *Nat Genet* 38:337–42

Sugarman JL, Fluhr JW, Fowler AJ, Bruckner T, Diepgen TL, Williams ML (2003) The objective severity assessment of atopic dermatitis score: an objective measure using permeability barrier function and stratum corneum hydration with computer-assisted estimates for extent of disease. *Arch Dermatol* 139:1417–22

Tanaka A, Tanaka T, Suzuki H, Ishii K, Kameyoshi Y, Hide M (2006) Semi-purification of the immunoglobulin E-sweat antigen acting on mast cells and basophils in atopic dermatitis. *Exp Dermatol* 15:283–90

Tomita Y, Akiyama M, Shimizu H (2005) Stratum corneum hydration and flexibility are useful parameters to indicate clinical severity of congenital ichthyosis. *Exp Dermatol* 14:619–24

Weidinger S, Illig T, Baurecht H, Irvine AD, Rodriguez E, Diaz-Lacava A *et al.* (2006) Loss-of-function variations within the filaggrin gene predispose for atopic dermatitis with allergic sensitizations. *J Allergy Clin Immunol* 118:214–9

Yamamoto Y (1994) Measurement and analysis of skin electrical impedance. *Acta Derm Venereol* 185:34–8
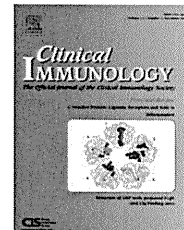
Noncollagenous 16A domain of type XVII collagen-reactive CD4 + T cells play a pivotal role in the development of active disease in experimental bullous pemphigoid model

Hideyuki Ujiie*, [1], Akihiko Shibaki, Wataru Nishie, Satoru Shinkuma, Reine Moriuchi, Hongjiang Qiao, Hiroshi Shimizu*

Department of Dermatology, Hokkaido University Graduate School of Medicine, Sapporo 060-8638, Japan

Abstract   Bullous pemphigoid (BP), the most common autoimmune blistering disease, is caused by autoantibodies against type XVII collagen (COL17). We recently demonstrated that CD4+ T cells were crucial for the production of anti-COL17 IgG and for the development of the BP phenotype by using a novel active BP mouse model by adoptively transferring immunized splenocytes into immunodeficient COL17-humanized mice. Noncollagenous 16A (NC16A) domain of COL17 is considered to contain the main pathogenic epitopes of BP, however, the pathogenicity of COL17 NC16A-reactive CD4+ T cells has never been elucidated. To address this issue, we modulated the immune responses against COL17 in active BP model by using anti-CD40 ligand (CD40L) monoclonal antibody MR1, an inhibitor of the CD40–CD40L interaction, in various ways. First, we show the essential role of CD4+ T cells in the model by showing that CD4+ T cells isolated from wild-type mice immunized with human COL17 enabled naïve B cells to produce anti-COL17 NC16A IgG in vivo. Second, we show that the activation of anti-COL17 NC16A IgG-producing B cells via CD40–CD40L interaction was completed within 5 days after the adoptive transfer of immunized splenocytes. Notably, a single administration of MR1 at day 0 was enough to inhibit the production of anti-COL17 NC16A IgG and to diminish skin lesions despite the presence of restored anti-COL17 IgG at the later stage. In contrast, the delayed administration of MR1 failed to inhibit the production of anti-COL17 NC16A IgG and the development of the BP phenotype. These results

1. Introduction

Bullous pemphigoid (BP) is the most common autoimmune blistering disorder. Clinically, tense blisters, erosions and crusts with itchy urticarial plaques and erythema develop on the entire body. Histologically, subepidermal blisters associated with inflammatory cell infiltration in the dermis are observed. BP is induced by autoantibodies against type XVII collagen (COL17, also called BP180 or BPAG2), a hemidesmosomal protein which spans the lamina lucida and projects into the lamina densa of the epidermal basement membrane zone (BMZ) [1–6]. The juxtamembranous noncollagenous 16A (NC16A) domain is considered to contain the main pathogenic epitopes on COL17, although BP patients' sera can also react with other parts [7–9].

Recently, we developed a novel active BP mouse model by adoptively transferring wild-type (WT) splenocytes immunized by human COL17 (hCOL17)-expressing transgenic (Tg) skin-grafting into $Rag\text{-}2^{-/-}/COL17^{m-/-,h+}$ ($Rag\text{-}2^{-/-}/COL17$-humanized) mice that express hCOL17 in the skin and lack both T and B cells [10]. The recipient mice accepted transferred splenocytes and produced high titers of anti-hCOL17 IgG in vivo for more than 10 weeks after the adoptive transfer, while circulating anti-hCOL17 NC16A IgG titer decreased in a short period for unknown reasons [10]. They developed blisters and erosions corresponding to clinical, histological and immunopathological features of BP [10]. This new active BP model enables us to observe the dynamic immune reactions induced by pathogenic antibodies against hCOL17 molecule.

In BP, the presence of autoreactive CD4$^+$ T cells has been reported [11–13]. Particular MHC class II alleles occur more frequently in BP patients [14]. These findings indicated the contribution of CD4$^+$ T cells to the pathogenesis of BP. Generally, the production of IgG by B cells requires the help of CD4$^+$ T cells [15–17]. Our previous study demonstrated that CD4$^+$ T cells were crucial for the production of anti-hCOL17 IgG and for the development of the BP phenotype because both the depletion of CD4$^+$ T cells from immunized splenocytes, and the administration of cyclosporin A significantly suppressed the pathogenic IgG production and diminished the disease severity [10]. However, the pathogenicity of COL17 NC16A-reactive CD4$^+$ T cells has never been elucidated. To address this issue, we modulated the CD4$^+$ T cell function in active BP model by administering anti-CD40L monoclonal antibody MR1 [18] in various ways, and observed the phenotypic changes of the treated mice.

CD40 ligand (CD40L) is a costimulatory molecule which is transiently expressed on the surface of activated CD4$^+$ T cells and which binds to CD40 on antigen-presenting cells including B cells. CD40–CD40L interaction is crucial for the proliferation and differentiation of B cells into immunoglobulin-secreting plasma cells and for the formation of humoral memory [19].

Immunosuppressive effects of anti-CD40L monoclonal antibody have been shown in some T-cell-mediated antibody-induced autoimmune animal models, such as experimental autoimmune myasthenia gravis [20], and pemphigus vulgaris [21, 22]. In this study, we demonstrate that COL17 NC16A-reactive CD4$^+$ T cells play a pivotal role in the development of BP through the CD40–CD40L interaction at an early stage of the disease in active BP model, which suggests that COL17 NC16A-reactive CD4$^+$ T cell is a promising therapeutic target for BP.

2. Materials and methods

2.1. Mice

C57BL/6J mice were purchased from Clea Japan. $Rag\text{-}2^{-/-}/COL17^{m-/-,h+}$ mice which carry the homozygous null mutations of both the $Rag\text{-}2$ and mouse Col17 genes and the transgene of human COL17 were generated by crossing $Rag\text{-}2^{-/-}$ mice (C57BL/6 background) with $COL17^{m-/-,h+}$ (COL17-humanized) mice (C57BL/6 background) as described previously [10]. All animal procedures were conducted according to guidelines of the Hokkaido University Institutional Animal Care and Use Committee under an approved protocol.

2.2. Induction of active BP by adoptive transfer of immunized splenocytes

Immunization of WT mice by hCOL17-expressing Tg skin graft was performed according to the method reported previously [10, 23]. After the confirmation of anti-hCOL17 IgG production at 5 weeks after skin grafting by indirect immunofluorescence (IF) analysis using normal human skin, splenocytes were isolated and pooled from several Tg skin-grafted immunized WT mice and administered into $Rag\text{-}2^{-/-}/COL17$-humanized mice by intravenous injection into the tail vain at 1.5–2.0×10^8 splenocytes in 500 μL PBS per mouse [10, 24].

2.3. Evaluation of active BP model mice

Weekly, the recipient mice were examined for general condition and cutaneous lesions (i.e., erythema, blisters, erosions, crusts and hair loss). Extent of skin disease was scored as follows: 0, no lesions; 1, lesions on less than 10% of the skin surface; 2, lesions on 10–20% of the skin surface; 3, lesions on 20–40% of the skin surface; 4, lesions on 40–60% of the skin surface; 5, lesions on more than 60% of the skin surface, as previously described [10]. Serum samples were also obtained from recipient mice weekly and assayed by indirect IF microscopy and hCOL17 NC16A ELISA as previously described [10]. The ELISA index value was defined by the following formula: index = (OD$_{450}$ of tested serum − OD$_{450}$ of negative control) / (OD$_{450}$ of positive control − OD$_{450}$ of

negative control)×100 [10]. Biopsies of lesional skin were obtained for light microscopy (H&E), and for direct IF using FITC-conjugated antibody against mouse IgG (Jackson ImmunoResearch Laboratories, West Grove, PA) and C3 (Cappel; Valeant Pharmaceuticals, Costa Mesa, CA).

2.4. Isolation of CD4$^+$ T cells or CD45R$^+$ B cells from splenocytes in mice

To examine the pathogenic role of CD4$^+$ T cells in active BP model, we isolated CD4$^+$ T cells from splenocytes of Tg skin-grafted WT mice by using a CD4$^+$ T cell isolation kit (Miltenyi Biotec, Bergisch Galdbach, Germany). 0.5 to 8×10^7 CD4$^+$ T cells were mixed with 2.0×10^8 naïve splenocytes from WT mice and adoptively transferred to Rag-2$^{-/-}$/COL17-humanized mice. In another experiment, CD45R$^+$ B cells were isolated from Tg skin-grafted WT mice by using CD45R MicroBeads (Miltenyi Biotec). 0.4×10^8 of CD45R$^+$ B cells were transferred to Rag-2$^{-/-}$/COL17-humanized mice. The isolation of CD4$^+$ T cells and CD45R$^+$ B cells was confirmed by flow cytometric analysis on FACSAria (BD Bioscience Pharmingen) using monoclonal antibodies purchased from BD Biosciences Pharmingen: H129.19-FITC (anti-CD4) and RA3-6B2-PE (anti-CD45R/B220).

2.5. In vivo monoclonal antibody treatment

Rag-2$^{-/-}$/COL17-humanized recipients that were adoptively transferred with immunized splenocytes were intraperitoneally injected with 500 μg hamster monoclonal antibody MR1 specific to mouse CD40L (Taconic Farms, Hudson, NY) or an equivalent amount of control hamster IgG (Rockland Immunochemicals, Gilbertsville, PA) at days 0, 2 and 6 after the adoptive transfer of immunized splenocytes as previously described [21], with some minor modifications. In a delayed treatment experiment, MR1 was injected at days 13, 16 and19 after the adoptive transfer. Some recipient mice were injected with 500 μg of MR1 just once on one of days 1 to 5 after the adoptive transfer, respectively. To investigate the immune responses in active BP model modulated by early single administration of MR1, 1000 μg of MR1 was injected into recipient mice at day 0 soon after the adoptive transfer. All treated mice were carefully observed for at least ten weeks after the adoptive transfer.

2.6. ELISPOT assay

ELISPOT assay was performed as previously described [10, 24]. Polyvinylidene-difluoride-bottomed 96-well multiscreen plates (Millipore) were coated with 30 μg/mL of recombinant hCOL17 NC16A protein. Splenocytes isolated from the Rag-2$^{-/-}$/COL17-humanized recipients were incubated on the plate at 37 °C in a 5% CO$_2$ incubator for 4 h. IgG bound to the membrane was visualized as spots, using alkaline-phosphatase-conjugated anti-mouse IgG antibody. The number of spots was counted using the ImmunoSpot S5 Versa Analyzer (Cellular Technology Ltd., Shaker Heights, OH), and the frequency of anti-hCOL17 NC16A IgG-producing B cells was defined as the number of spots in 10^5 mononuclear cells.

2.7. Statistical analysis

Data expressed as mean±standard error of means were analyzed using Student's t-test. We considered P values of less than 0.05 as significant.

3. Results

3.1. CD4$^+$ T cells are required for the production of pathogenic antibody in active BP model

We previously reported that CD4$^+$ − but not CD8$^+$ − T cells are crucial for the production of anti-hCOL17 IgG and for the development of the BP phenotype in active BP model [10]. To further analyze the contribution of CD4$^+$ T cells, we additionally conducted two experiments. First, mixed transfer into Rag-2$^{-/-}$/COL17-humanized mice of 4 or 8×10^7 CD4$^+$ T cells from WT splenocytes immunized by hCOL17-expressing Tg skin-grafting and 2×10^8 naïve splenocytes from unimmunized WT mice produced high titers of anti-hCOL17 NC16A IgG and severe BP skin changes associated with linear deposition of IgG at the BMZ. In contrast, reducing the number of CD4$^+$ T cells (0.5×10^7) failed to produce such titers and skin changes (n=3, respectively; Fig. 1). Second, we isolated CD45R$^+$ B cells from immunized splenocytes and adoptively transferred 0.4×10^8 of those cells into Rag-2$^{-/-}$/COL17-humanized recipients (n=3), which produced quite low levels of anti-hCOL17 NC16A IgG (mean index value of ELISA at day 9: 3.28) and no skin changes (not shown). These results show that the production of anti-hCOL17 NC16A IgG by B cells and the development of BP skin changes in active BP model depend heavily on immunized CD4$^+$ T cells.

3.2. Anti-CD40L monoclonal antibody suppresses the production of anti-hCOL17 IgG and skin changes in active BP model

To investigate the precise mechanism of the activation of B cells by immunized CD4$^+$ T cells in active BP model, we assessed the role of CD40–CD40L interaction. Rag-2$^{-/-}$/COL17-humanized recipients were injected intraperitoneally with 500 μg of monoclonal antibody MR1 specific to mouse CD40L or an equivalent dose of hamster IgG as a control on days 0, 2 and 6 after the adoptive transfer of immunized splenocytes (n=6, respectively). All the control Rag-2$^{-/-}$/COL17-humanized recipients produced high titers of IgG against BMZ of normal human skin, which reflects the presence of anti-hCOL17 IgG, and those against hCOL17 NC16A, as previously reported [10]. In contrast, the production of those antibodies was almost completely inhibited in all the mice that were injected with MR1, and the inhibitory effect persisted for more than 10 weeks (Figs. 2A, B). The control mice developed patchy hair loss associated with erythema around day 14 after the adoptive transfer. Then, blisters and erosions spontaneously developed in the depilated areas on the trunk (Fig. 3A). Disease severity, scored by the percent of skin surface with the BP phenotype [10, 25], gradually increased, plateauing 7 weeks after the transfer in the control mice (Fig. 3G). In contrast, none of the MR1-
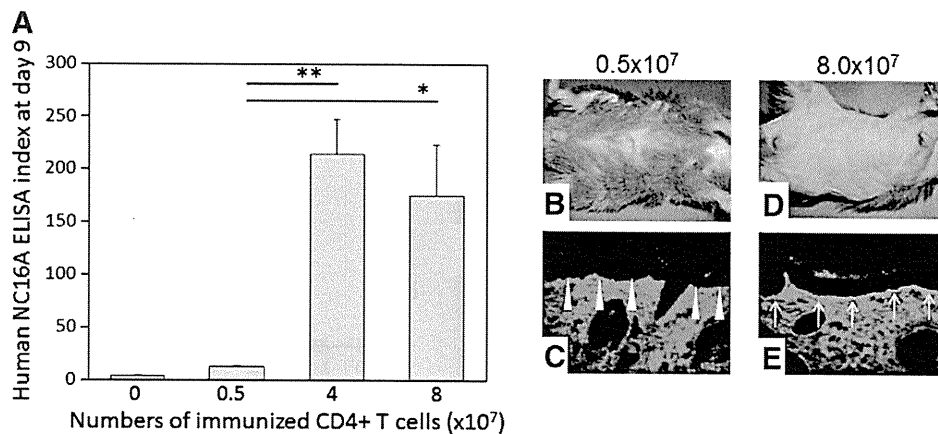
A

Fig. 1 Immunized CD4⁺ T cells can activate naïve B cells to produce anti-hCOL17 NC16A IgG in vivo. (A) CD4⁺ T cells isolated from WT splenocytes immunized by hCOL17-expressing Tg skin-grafting were mixed with naïve splenocytes from untreated WT mice, and were adoptively transferred into $Rag\text{-}2^{-/-}$/COL17-humanized mice (n=3, respectively). Mice transferred with 4 or 8×10^7 immunized CD4⁺ T cells mixed with naïve splenocytes produce significantly higher levels of anti-hCOL17 NC16A IgG than with 0.5×10^7 CD4⁺ T cells mixed with naïve splenocytes (*$P<0.05$, **$P<0.01$). Mice transferred with 0.5×10^7 of immunized CD4⁺ T cells and naïve splenocytes show no skin changes (B) or deposition of IgG (C). In contrast, mice transferred with 8×10^7 immunized CD4⁺ T cells and naïve splenocytes develop severe BP skin changes (D) associated with linear deposition of IgG at the BMZ (E).

treated mice developed any skin lesions (Figs. 3D, G). Histopathological analysis of the skin revealed the dermal–epidermal separation that is associated with mild inflammatory cell infiltration in control mice (Fig. 3B), whereas there were no histopathological changes in MR1-treated mice (Fig. 3E). Direct IF analysis of lesional skin revealed linear deposition of IgG (Fig. 3C) at the BMZ in the control mice, whereas IgG deposition was absent or faint in the MR1-treated mice (Fig. 3F). We also examined the number of splenocytes which produced anti-hCOL17 NC16A IgG by enzyme-linked immunospot assay at day 9. In the control, 226.5±25.0 cells in 10^5 splenocytes produced anti-hCOL17 NC16A IgG, whereas only 9.0±3.0 cells in 10^5 splenocytes produced them in the mice treated with MR1 (n=3, respectively; Fig. 3H). Thus, preventive and repetitive administration of MR1 can continuously suppress

the production of anti-hCOL17 IgG and skin changes in active BP model.

3.3. Anti-CD40L monoclonal antibody shows no effects in mice with established active BP

To examine the effect of MR1 in mice with producing IgG against hCOL17 and hCOL17 NC16A, 500 μg of MR1 or the equivalent dose of normal hamster IgG were administered into active BP model at days 13, 16 and 19 after the adoptive transfer of splenocytes (n=4, respectively). There were no significant differences in the titers of anti-hCOL17 or anti-hCOL17 NC16A IgG, nor in disease severity in both groups at more than 10 weeks after the adoptive transfer (Fig. 4).
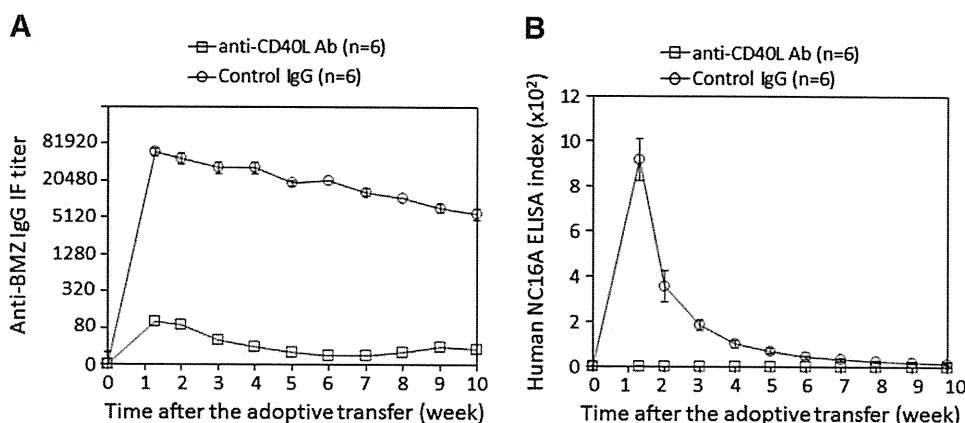

Fig. 2 Anti-CD40L monoclonal antibody strongly suppresses the production of anti-hCOL17 and anti-hCOL17 NC16A IgG and in active BP model. $Rag\text{-}2^{-/-}$/COL17-humanized recipients were injected intraperitoneally with monoclonal antibody specific to mouse CD40L (MR1) or the equivalent dose of control hamster IgG on day 0, 2 and 6 after the adoptive transfer of immunized splenocytes (n=6, respectively). All the $Rag\text{-}2^{-/-}$/COL17-humanized recipients that were injected with control IgG produce significantly high titers of IgG against hCOL17 (BMZ of normal human skin) and hCOL17 NC16A, while the production of those antibodies is almost completely inhibited in all mice injected with MR1 (A, B) $P<0.01$ from day 9 to day 70 in both graphs.
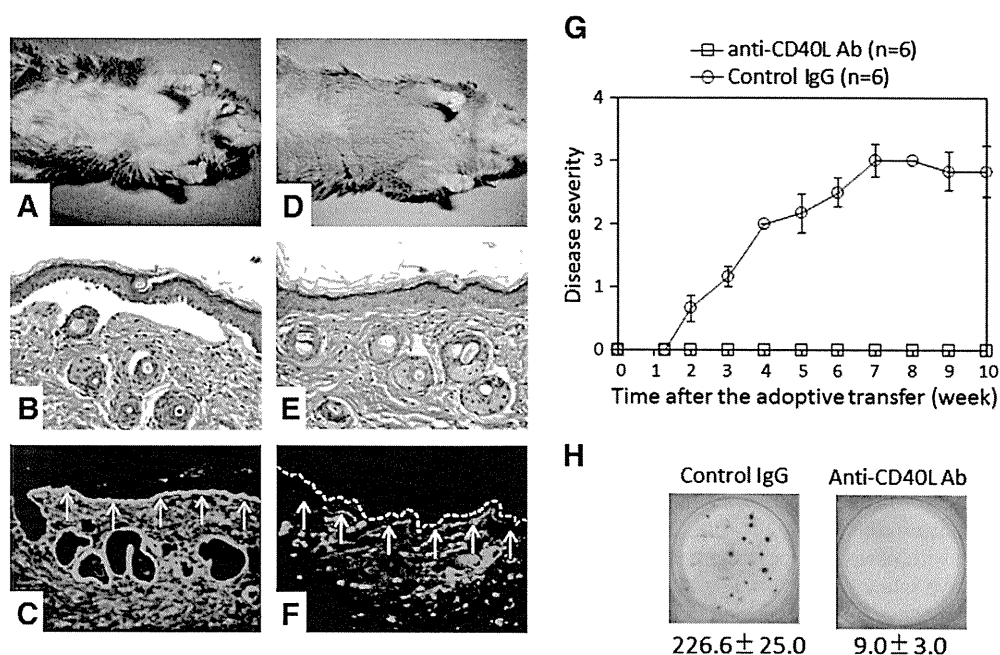
G

-□- anti-CD40L Ab (n=6)
-○- Control IgG (n=6)

Disease severity / Time after the adoptive transfer (week)

H

Control IgG   Anti-CD40L Ab

226.6±25.0   9.0±3.0

Fig. 3   Skin changes are completely inhibited in the MR1-treated mice. (A) Control $Rag-2^{-/-}$/COL17-humanized recipients develop blisters and erosions spontaneously develop in the depilated areas on the trunk (n=6). (B) Histopathologic analysis of the skin reveals the dermal–epidermal separation associated with mild inflammatory cell infiltration in the control group. (C) Direct IF analysis of lesional skin demonstrates linear deposition of IgG at the BMZ in control mice. None of the MR1-treated mice demonstrate any skin lesions (D) or histopathologic changes (E) (n=6). (F) No or faint IgG deposition is detected in the treated mice. (G) Disease severity, which was scored by the percentage of affected skin surface area, gradually increases and plateaus at 7 weeks after the adoptive transfer in the control mice, whereas that is stably zero in the MR1-treated mice ($P<0.05$ at day 14, $P<0.01$ from day 21 to day 70) (H) Enzyme-linked immunospot assay using recombinant hCOL17 NC16A protein at day 9 after the adoptive transfer. In contrast to the control, very few spots are seen in the well of the MR1-treated splenocytes. The number of anti-hCOL17 NC16A IgG-producing B cells is displayed per 10^5 cells in the spleen (n=3, respectively).

These findings show that delayed administration of MR1 fails to diminish the disease activity in established active BP mice.

3.4. Activation of anti-hCOL17 NC16A IgG-producing B cells via CD40–CD40L interaction is completed within five days after the adoptive transfer of immunized splenocytes

Since the delayed administration of MR1 failed to diminish the disease activity, we considered that the timing of T–B interaction via the CD40–CD40L pathway after the adoptive transfer needed to be elucidated. Single injections of 1000 µg of MR1 at days 1 to 5 after the adoptive transfer of immunized splenocytes into the $Rag-2^{-/-}$/COL17-humanized recipients were administered (n=4, respectively). Injection of MR1 at day 1, day 2 or day 3 strongly inhibited the production of anti-h COL17 NC16A IgG in recipients (Fig. 5A). The effects of MR1 successively decreased if the treatment was initiated at day 4 or day 5. Anti-hCOL17 NC16A IgG titer and disease severity of the recipients treated at day 5 were similar to those in active BP model without MR1 treatment (mean index value of anti-hCOL17 NC16A IgG at day 9: 765.3 vs. 918.97, $P>0.05$; mean disease severity at day 35: 3.00 vs. 2.16, $P>0.05$) (Figs. 2B, 3G and 5). Thus, the activation of anti-hCOL17 NC16A IgG-producing B cells via CD40–

CD40L interaction is completed within 5 days after the adoptive transfer of immunized splenocytes in active BP model.

3.5. Anti-hCOL17 IgG restored after the early single administration of anti-CD40L monoclonal antibody do not contain anti-hCOL17 NC16A IgG, and only weak pathogenicity is shown

The results above suggested that the early short-term effect of MR1 was sufficient to inhibit the production of anti-hCOL17 NC16A IgG. To observe the phenotypic changes in active BP model without the presence of anti-hCOL17 NC16A IgG, we induced the transient immunosuppressive condition in $Rag-2^{-/-}$/COL17-humanized recipients by single injections of 1000 µg of MR1 at day 0 (n=6). The production of anti-hCOL17 IgG in treated mice gradually recovered to levels similar to those in the control mice without MR1-treatment at 7 weeks after the adoptive transfer (Fig. 6A), but the restored IgG did not contain anti-hCOL17 NC16A IgG (Fig. 6B). The disease severity of the treated mice slowly increased but was significantly lower than that of the controls (Fig. 6C). Each of the IgG subclasses (IgG1, IgG2b, IgG2c, IgG3) against hCOL17 showed similar titers between an MR1-treated group and an untreated group at 10 weeks after the adoptive transfer (not shown). Although 3 out of 6 treated mice showed distinct deposition of C3, they

A

-□- anti-CD40L Ab delay (n=4)
-○- Control active BP model (n=4)

Anti-BMZ IgG IF titer

81920
20480
5120
1280
320
80
0

0 1 2 3 4 5 6 7 8 9 10

Time after the adoptive transfer (week)

B

-□- anti-CD40L Ab delay (n=4)
-○- Control active BP model (n=4)

Human NC16A ELISA index (×10²)

12
10
8
6
4
2
0

0 1 2 3 4 5 6 7 8 9 10

Time after the adoptive transfer (week)

C

-□- anti-CD40L Ab delay (n=4)
-○- Control active BP model (n=4)

Disease severity

5
4
3
2
1
0

0 1 2 3 4 5 6 7 8 9 10
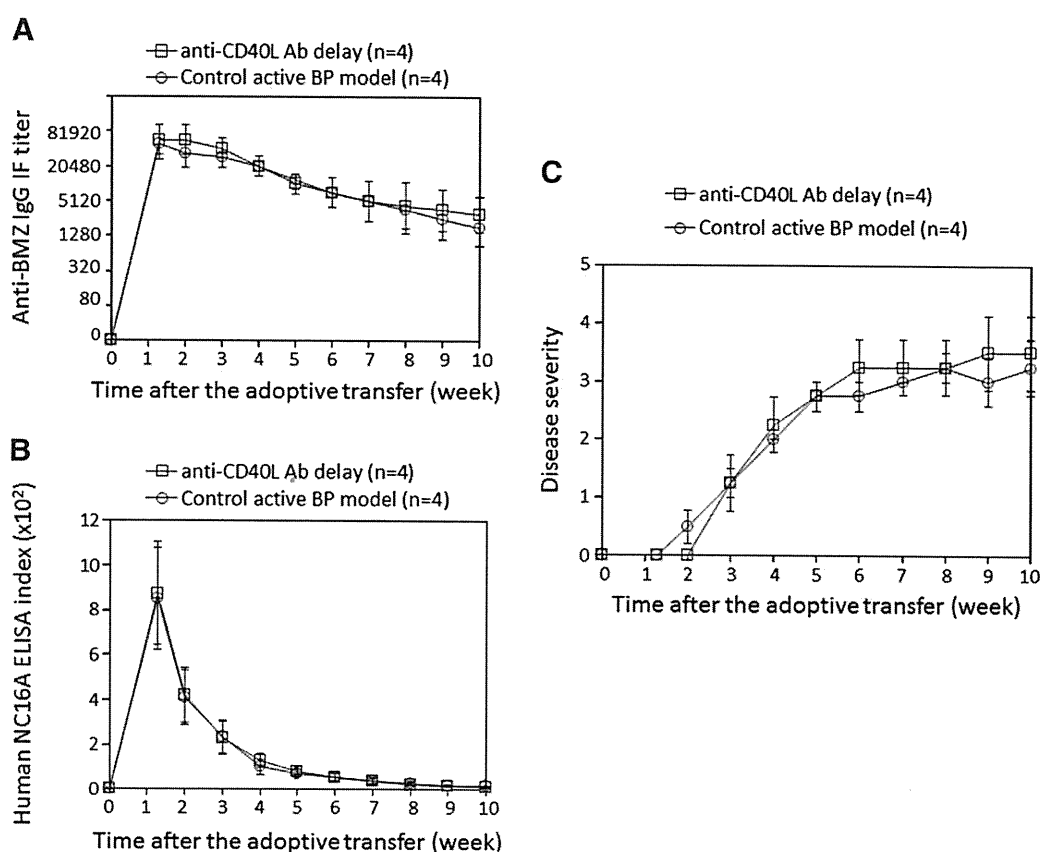
Time after the adoptive transfer (week)

Fig. 4 Delayed treatment with anti-CD40L monoclonal antibody shows no effects in mice with established active BP. MR1 or control hamster IgG was injected into active BP model at days 13, 16 and 19 after the adoptive transfer of immunized splenocytes (n=4, respectively). There are no significant differences in the titers of anti-hCOL17 IgG (A) or anti-hCOL17 NC16A IgG (B), and in disease severity (C) between the groups. $P>0.05$.

developed only mild skin changes (Fig. 6D). Thus, anti-hCOL17 IgG restored after the transient blockade of CD40–CD40L interaction contain no anti-hCOL17 NC16A IgG and show only weak pathogenicity. This strongly suggests that hCOL17 NC16A-reactive CD4$^+$ T cells play a crucial role in the development of BP lesions in active mouse model.

4. Discussion

This study has demonstrated the pivotal role of COL17 NC16A-reactive CD4$^+$ T cells in BP induction for the first time by using active BP mouse model. We first demonstrated the pathogenic role of CD4$^+$ T cells in active BP model by showing that CD4$^+$ T cells immunized by hCOL17-expressing Tg-skin grafting could activate unimmunized B cells to produce anti-hCOL17 NC16A IgG. We also showed that immunized CD45R$^+$ B cells needed the coexistence of activated CD4$^+$ T cells to produce those IgG. These results suggest that the interaction between activated hCOL17-reactive T cells and B cells is essential for the production of anti-hCOL17 IgG. Administrations of anti-CD40L monoclonal antibody have previously demonstrated the strong suppression of humoral immune responses against autoantigens in some

T-cell-mediated antibody-induced autoimmune animal models [20–22, 26]. Therefore, we considered that anti-CD40L monoclonal antibody may be utilized for the modulation of immune responses in active BP model.

Blockade of CD40–CD40L interaction by anti-CD40L monoclonal antibody (MR1) continuously suppressed the production of anti-hCOL17 NC16A IgG and the development of the BP phenotype in active BP model when MR1 was repetitively administered close to the time of adoptive transfer of immunized splenocytes. Although the production of anti-hCOL17 IgG detected by indirect IF study using normal human skin was not completely suppressed by MR1 treatment, ELISA revealed an absence of anti-hCOL17 NC16A IgG, resulting in the prevention of BP skin changes. Enzyme-linked immunospot assay demonstrated quite a small number of anti-hCOL17 NC16A IgG-producing B cells in the spleens of the MR1-treated mice.

Because the crucial role of B cell activation via CD40–CD40L interaction was elucidated at the initial stage of active BP model, we then tried to examine the effects of MR1 at the late stage of active BP model. Since the model starts to produce anti-hCOL17 and anti-hCOL17 NC16A IgG within a week after the adoptive transfer if no immunosuppressive treatment is added [10], we injected MR1 at days 13, 16
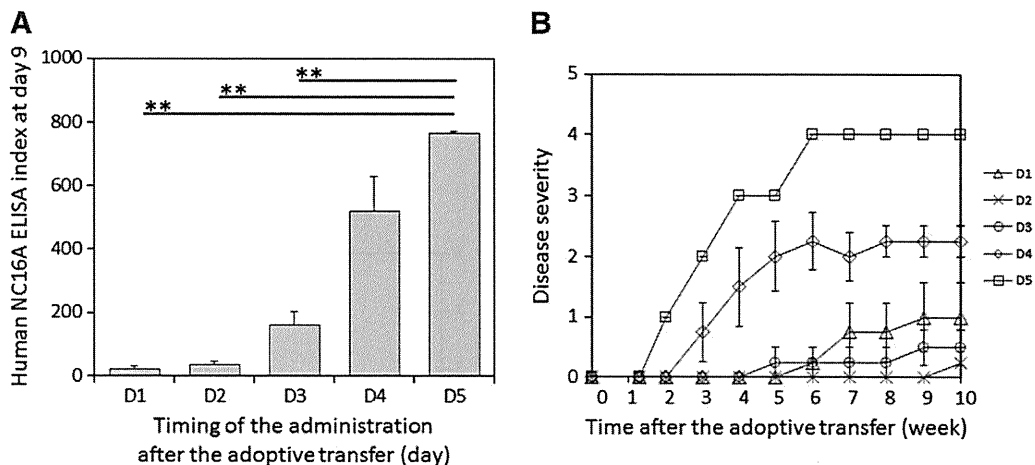
Fig. 5 Activation of anti-hCOL17 NC16A IgG-producing B cells via CD40–CD40L interaction is established within 5 days after the adoptive transfer of immunized splenocytes. Rag-2$^{-/-}$/COL17-humanized recipients were injected with MR1 just once between days 1 and 5 after the adoptive transfer of immunized splenocytes (n=4, respectively). (A) MR1-treatments at day 1, day 2 or day 3 significantly suppress the titers of anti-hCOL17 NC16A IgG at day 9 compared with those at day 5 (**$P<0.01$). The effect of MR1 gradually decreases if the treatment is initiated late. The IgG titers at day 9 of the mice treated at day 5 are similar to those in active BP model without MR1 treatment (Fig. 2B) (mean index value: 765.3 vs. 918.97, $P>0.05$). (B) Skin changes are strongly suppressed if MR1-treatment is initiated before day 3 after the adoptive transfer. Disease severity of the recipients treated at day 5 is similar to those in active BP model without MR1 treatment (Fig. 3G) (mean disease severity at day 35: 3.00 vs. 2.16, $P>0.05$).

and 19 after the adoptive transfer (delayed treatment). No therapeutic effects were observed in mice with delayed treatment. This result indicates that the CD40–CD40L interaction is not required once the disease is established in active BP model. Similarly, delayed MR1-treatment was unable to suppress the titer of pathogenic antibody in an established pemphigus vulgaris model [21]. Meanwhile, delayed treatment can prevent relapses of ongoing diseases or can halt disease progression in models of multiple sclerosis [27], lupus nephritis [28, 29] and myasthenia gravis [20]. A possible mechanism of those therapeutic effects is the inhibition of epitope spreading. In experimental autoimmune encephalomyelitis, anti-CD40L monoclonal antibody treatment acts in part by inhibiting the expansion and/or differentiation of Th1 effector cells specific to relapse-associated epitopes [27]. Epitope spreading has also been reported in BP patients [30–32] and in an hCOL17-expressing Tg skin-grafting mouse model [33] although it is still unclear whether antibodies against hCOL17 – other than those against the NC16A domain – are pathogenic. Hence, the efficacy of anti-CD40L antibody treatment on epitope spreading in BP seems an interesting line of investigation.

Furthermore, we revealed that the activation of anti-hCOL17 NC16A IgG-producing B cells via CD40–CD40L interaction was completed within 5 days after the adoptive transfer of immunized splenocytes. This suggests that the short-term effect of MR1 at the early stage of active BP is sufficient to inhibit the production of anti-hCOL17 NC16A IgG. Therefore, we tried to investigate the immune responses at the late stage of active BP model under the condition of no anti-hCOL17 IgG by means of early administration of a single dose of MR1. As shown in Figs. 6A and B, the production of

anti-hCOL17 NC16A IgG was durably suppressed by the early single MR1-treatment, while the production of anti-hCOL17 IgG gradually recovered. Previous study using active pemphigus vulgaris model demonstrated that MR1-treatment could induce tolerance to desmoglein 3 in the treated mice and the tolerance was transferable [21]. Our results suggest that the MR1-treatment induced immune tolerance to some antigens including hCOL17 NC16A in the treated mice, which induced the durable suppression of the anti-hCOL17 NC16A IgG production. Some other hCOL17-reactive CD4$^+$ T cells which escaped the tolerance-induction might activate B cells as the effect of the MR1-treatment wore off. Of note, the treated mice developed only mild skin changes despite the high titers of restored anti-hCOL17 IgG in the late stage. In this setting, some mice showed the distinct deposition of complements as well as IgG at the BMZ but developed only mild skin changes. Complement activation is considered important in the pathogenesis of BP [34–36], while anti-hCOL17 IgG from BP patients has been proven to reduce the content of hemidesmosomal COL17 and weaken the adhesion of hemidesmosomes to the lamina densa without complements [37]. Thus, the significance of complement activation in the pathogenesis of BP remains controversial. As we reported previously [10], untreated active BP model demonstrates a trend in which the disease severity starts to decrease around 12 weeks after the adoptive transfer. The results shown in Fig. 6 demonstrate that anti-hCOL17 NC16A IgG is the major pathogenic antibody and able to cause severe skin changes for more than 10 weeks after the adoptive transfer. In addition, they indicate that some antibodies against hCOL17 other than against the NC16A domain have weak pathogenicity and partially sustain the disease activity in the late stage of active BP
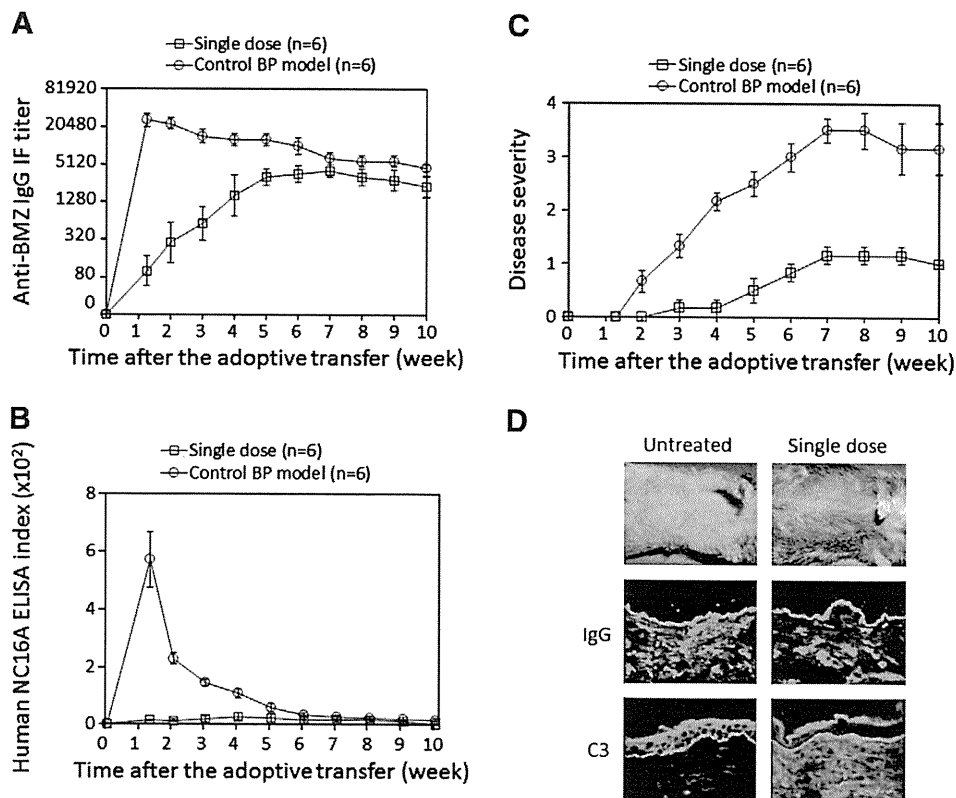
A

B

C

D

Fig. 6 Early single dose of anti-CD40L monoclonal antibody inhibits the production of anti-hCOL17 NC16A IgG, while the production of anti-hCOL17 IgG is recovered in the late stage. 1000 μg of MR1 was injected into $Rag\text{-}2^{-/-}$/COL17-humanized recipients at day 0 just once (n=6). (A) Anti-hCOL17 IgG titer gradually increases and reaches to a level similar to that of control active BP model at 7 weeks after the adoptive transfer ($P<0.01$ at days 9, 14 and 21; $P<0.05$ at days 28, 35 and 42; $P>0.05$ at days 0, 49, 56, 63 and 70). (B) Anti-hCOL17 NC16A IgG titers are significantly lower in the treated mice than those in the controls ($P<0.01$ at days 9, 14, 21 and 28). (C) Disease severity of the treated mice slowly increases but is significantly lower than that of the controls ($P<0.05$ at day 14; $P<0.01$ from day 21 to 70). (D) Some of the treated mice show the distinct deposition of C3 and have developed just a mild skin change (Fig. 6D).

model. In conclusion, this study suggests that COL17 NC16A-reactive CD4$^+$ T cells play a pivotal role in the pathogenesis of active BP model via the CD40–CD40L interaction.

Conflict of interest statement

The author(s) declare that there are no conflicts of interest.

Acknowledgments

References

[1] L.A. Diaz, H. Ratrie III, W.S. Saunders, S. Futamura, H.L. Squiquera, G.J. Anhalt, et al., Isolation of a human epidermal cDNA corresponding to the 180-kD autoantigen recognized by bullous pemphigoid and herpes gestationis sera. Immunolocalization of this protein to the hemidesmosome, J. Clin. Invest. 86 (1990) 1088–1094.

[2] G.J. Giudice, D.J. Emery, L.A. Diaz, Cloning and primary structural analysis of the bullous pemphigoid autoantigen BP180, J. Invest. Dermatol. 99 (1992) 243–250.

[3] S.B. Hopkinson, K.S. Riddelle, J.C. Jones, Cytoplasmic domain of the 180-kD bullous pemphigoid antigen, a hemidesmosomal component: molecular and cell biologic characterization, J. Invest. Dermatol. 99 (1992) 264–270.

[4] A. Ishiko, H. Shimizu, A. Kikuchi, T. Ebihara, T. Hashimoto, T. Nishikawa, Human autoantibodies against the 230-kD bullous pemphigoid antigen (BPAG1) bind only to the intracellular domain of the hemidesmosome, whereas those against the 180-kD bullous pemphigoid antigen (BPAG2) bind along the plasma membrane of the hemidesmosome in normal human and swine skin, J. Clin. Invest. 91 (1993) 1608–1615.

[5] C. Bedane, J.R. McMillan, S.D. Balding, P. Bernard, C. Prost, J.M. Bonnetblanc, et al., Bullous pemphigoid and cicatricial pemphigoid autoantibodies react with ultrastructurally separable epitopes on the BP180 ectodomain: evidence that BP180

spans the lamina lucida, J. Invest. Dermatol. 108 (1997) 901–907.

[6] J.R. McMillan, M. Akiyama, H. Shimizu, Epidermal basement membrane zone components: ultrastructural distribution and molecular interactions, J. Dermatol. Sci. 31 (2003) 169–177.

[7] G.J. Giudice, D.J. Emery, B.D. Zelickson, G.J. Anhalt, Z. Liu, L.A. Diaz, Bullous pemphigoid and herpes gestationis autoanti-bodies recognize a common non-collagenous site on the BP180 ectodomain, J. Immunol. 151 (1993) 5742–5750.

[8] D. Zillikens, P.A. Rose, S.D. Balding, Z. Liu, M. Olague-Marchan, L.A. Diaz, et al., Tight clustering of extracellular BP180 epitopes recognized by bullous pemphigoid autoanti-bodies, J. Invest. Dermatol. 109 (1997) 573–579.

[9] Y. Tsuji-Abe, M. Akiyama, Y. Yamanaka, T. Kikuchi, K.C. Sato-Matsumura, H. Shimizu, Correlation of clinical severity and ELISA indices for the NC16A domain of BP180 measured using BP180 ELISA kit in bullous pemphigoid, J. Dermatol. Sci. 37 (2005) 145–149.

[10] H. Ujiie, A. Shibaki, W. Nishie, D. Sawamura, G. Wang, Y. Tateishi, et al., A novel active mouse model for bullous pem-phigoid targeting humanized pathogenic antigen, J. Immunol. 184 (2010) 2166–2174.

[11] L. Budinger, L. Borradori, C. Yee, R. Eming, S. Ferencik, H. Grosse-Wilde, et al., Identification and characterization of autoreactive T cell responses to bullous pemphigoid antigen 2 in patients and healthy controls, J. Clin. Invest. 102 (1998) 2082–2089.

[12] M.S. Lin, C.L. Fu, G.J. Giudice, M. Olague-Marchan, A.M. Lazaro, P. Stastny, et al., Epitopes targeted by bullous pemphi-goid T lymphocytes and autoantibodies map to the same sites on the bullous pemphigoid 180 ectodomain, J. Invest. Derma-tol. 115 (2000) 955–961.

[13] S. Thoma-Uszynski, W. Uter, S. Schwietzke, G. Schuler, L. Borradori, M. Hertl, Autoreactive T and B cells from bullous pemphigoid (BP) patients recognize epitopes clustered in dis-tinct regions of BP180 and BP230, J. Immunol. 176 (2006) 2015–2023.

[14] J.C. Delgado, D. Turbay, E.J. Yunis, J.J. Yunis, E.D. Morton, K. Bhol, et al., A common major histocompatibility complex class II allele HLA-DQB1* 0301 is present in clinical variants of pem-phigoid, Proc. Natl. Acad. Sci. U.S.A. 93 (1996) 8569–8571.

[15] M. Aoki-Ota, K. Tsunoda, T. Ota, T. Iwasaki, S. Koyasu, M. Amagai, et al., A mouse model of pemphigus vulgaris by adop-tive transfer of naive splenocytes from desmoglein 3 knockout mice, Br. J. Dermatol. 151 (2004) 346–354.

[16] A.G. Sitaru, A. Sesarman, S. Mihai, M.T. Chiriac, D. Zillikens, P. Hultman, et al., T cells are required for the production of blister-inducing autoantibodies in experimental epidermolysis bullosa acquisita, J. Immunol. 184 (2010) 1596–1603.

[17] G.X. Zhang, B.G. Xiao, M. Bakhiet, P. van der Meide, H. Wigzell, H. Link, et al., Both CD4⁺ and CD8⁺ T cells are essential to induce experimental autoimmune myasthenia gravis, J. Exp. Med. 184 (1996) 349–356.

[18] R.J. Noelle, M. Roy, D.M. Shepherd, I. Stamenkovic, J.A. Ledbetter, A. Aruffo, A 39-kDa protein on activated helper T cells binds CD40 and transduces the signal for cognate ac-tivation of B cells, Proc. Natl. Acad. Sci. U.S.A. 89 (1992) 6550–6554.

[19] A.L. Peters, L.L. Stunz, G.A. Bishop, CD40 and autoimmunity: the dark side of a great activator, Semin. Immunol. 21 (2009) 293–300.

[20] S.H. Im, D. Barchan, P.K. Maiti, S. Fuchs, M.C. Souroujon, Blockade of CD40 ligand suppresses chronic experimental my-asthenia gravis by down-regulation of Th1 differentiation and up-regulation of CTLA-4, J. Immunol. 166 (2001) 6893–6898.

[21] M. Aoki-Ota, M. Kinoshita, T. Ota, K. Tsunoda, T. Iwasaki, S. Tanaka, et al., Tolerance induction by the blockade of CD40/CD154 interaction in pemphigus vulgaris mouse model, J. Invest. Dermatol. 126 (2006) 105–113.

[22] M. Ohyama, T. Ota, M. Aoki, K. Tsunoda, R. Harada, S. Koyasu, et al., Suppression of the immune response against exogenous desmoglein 3 in desmoglein 3 knockout mice: an implication for gene therapy, J. Invest. Dermatol. 120 (2003) 610–615.

[23] E.B. Olasz, J. Roh, C.L. Yee, K. Arita, M. Akiyama, H. Shimizu, et al., Human bullous pemphigoid antigen 2 transgenic skin elicits specific IgG in wild-type mice, J. Invest. Dermatol. 127 (2007) 2807–2817.

[24] M. Amagai, K. Tsunoda, H. Suzuki, K. Nishifuji, S. Koyasu, T. Nishikawa, Use of autoantigen-knockout mice in developing an active autoimmune disease model for pemphigus, J. Clin. Invest. 105 (2000) 625–631.

[25] C. Sitaru, S. Mihai, C. Otto, M.T. Chiriac, I. Hausser, B. Dotterweich, et al., Induction of dermal-epidermal separa-tion in mice by passive transfer of antibodies specific to type VII collagen, J. Clin. Invest. 115 (2005) 870–878.

[26] C.M. Lanschuetzer, E.B. Olasz, Z. Lazarova, K.B. Yancey, Transient anti-CD40L co-stimulation blockade prevents immune responses against human bullous pemphigoid antigen 2: implications for gene therapy, J. Invest. Dermatol. 129 (2009) 1203–1207.

[27] L.M. Howard, A.J. Miga, C.L. Vanderlugt, M.C. Dal Canto, J.D. Laman, R.J. Noelle, et al., Mechanisms of immunotherapeutic intervention by anti-CD40L (CD154) antibody in an animal model of multiple sclerosis, J. Clin. Invest. 103 (1999) 281–290.

[28] S.L. Kalled, A.H. Cutler, S.K. Datta, D.W. Thomas, Anti-CD40 ligand antibody treatment of SNF1 mice with established ne-phritis: preservation of kidney function, J. Immunol. 160 (1998) 2158–2165.

[29] S.A. Quezada, M. Eckert, O.A. Adeyi, A.R. Schned, R.J. Noelle, C.M. Burns, Distinct mechanisms of action of anti-CD154 in early versus late treatment of murine lupus nephritis, Arthritis Rheum. 48 (2003) 2541–2554.

[30] G. Di Zenzo, F. Grosso, M. Terracina, F. Mariotti, O. De Pita, K. Owaribe, et al., Characterization of the anti-BP180 autoanti-body reactivity profile and epitope mapping in bullous pemphi-goid patients, J. Invest. Dermatol. 122 (2004) 103–110.

[31] G. Di Zenzo, S. Thoma-Uszynski, L. Fontao, V. Calabresi, S.C. Hofmann, T. Hellmark, et al., Multicenter prospective study of the humoral autoimmune response in bullous pemphigoid, Clin. Immunol. 128 (2008) 415–426.

[32] G. Di Zenzo, S. Thoma-Uszynski, V. Calabresi, L. Fontao, S.C. Hofmann, J.P. Lacour, et al., Demonstration of epitope-spreading phenomena in bullous pemphigoid: results of a pro-spective multicenter study, J. Invest. Dermatol. 131 (2011) 2271–2280.

[33] G. Di Zenzo, V. Calabresi, E.B. Olasz, G. Zambruno, K.B. Yan-cey, Sequential intramolecular epitope spreading of humoral responses to human BPAG2 in a transgenic model, J. Invest. Dermatol. 130 (2010) 1040–1047.

[34] Q. Li, H. Ujiie, A. Shibaki, G. Wang, R. Moriuchi, H.J. Qiao, et al., Human IgG1 monoclonal antibody against human colla-gen 17 noncollagenous 16A domain induces blisters via comple-ment activation in experimental bullous pemphigoid model, J. Immunol. 185 (2010) 7746–7755.

[35] Z. Liu, G.J. Giudice, S.J. Swartz, J.A. Fairley, G.O. Till, J.L. Troy, et al., The role of complement in experimental bullous pemphigoid, J. Clin. Invest. 95 (1995) 1539–1544.

[36] G. Wang, H. Ujiie, A. Shibaki, W. Nishie, Y. Tateishi, K. Kikuchi, et al., Blockade of autoantibody-initiated tissue damage by using recombinant fab antibody fragments against pathogenic autoantigen, Am. J. Pathol. 176 (2010) 914–925.

[37] H. Iwata, N. Kamio, Y. Aoyama, Y. Yamamoto, Y. Hirako, K. Owaribe, et al., IgG from patients with bullous pemphigoid de-pletes cultured keratinocytes of the 180-kDa bullous pemphi-goid antigen (type XVII collagen) and weakens cell attachment, J. Invest. Dermatol. 129 (2009) 919–926.
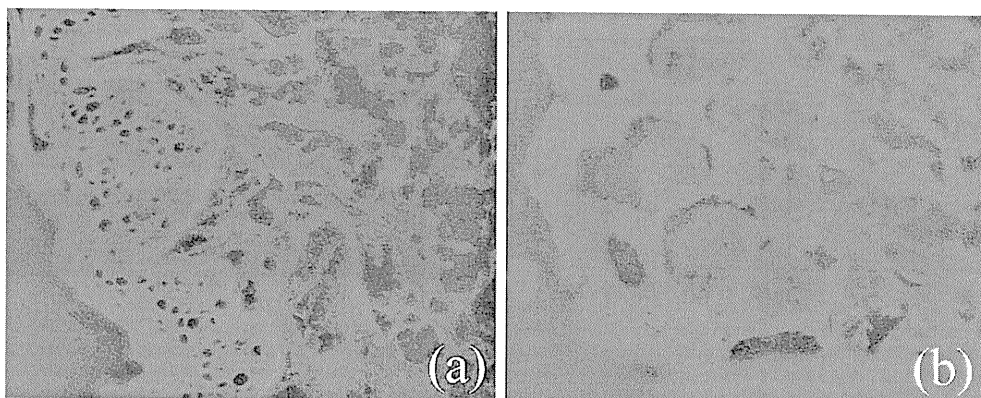
Fig. 2. Indirect immunofluoresence for collagen VII autoantibodies on normal skin (a) and collagen VII deficient skin (b) with serum from EBA patient, 200×.

We agree with the authors that more studies are indicated to determine the use of this test for monitoring disease activity in EBA patients. Similar studies in pemphigus patients with recombinant desmoglein 1 and 3 ELISA's reveal that the sera with identical titers of antibodies by IIF give variable results with ELISA [7]. Unless high titer sera are diluted, saturation of antibody–antigen reactions in ELISA may lead to false low positive ELISA index values to begin with. Such sera may not appear to show a decline in ELISA index values with treatment response [8]. We also have observed, in some pemphigus sera, that even though the IIF titers show a decline, ELISA index values still remain high. Therefore, we may have to use this ELISA with caution to monitor the disease.

References

[1] Saleh MA, Ishii K, Kim YJ, Murakami A, Ishii N, Hashimoto T, et al. Development of NC1 and NC2 domains of Type VII collagen ELISA for the diagnosis and analysis of the time course of epidermolysis bullosa acquisita patients. J Dermatol Sci 2011;62(3):169–75.

[2] Gammon WR, Briggaman RA, Inman III AO, Queen LL, Wheeler CE. Differentiating anti-lamina lucida and anti-sublamina densa anti-BMZ antibodies by indirect immunofluorescence on 1.0 M sodium chloride-separated skin. J Invest Dermatol 1984;82(2):139–44.

[3] Vodegel RM, de Jong MC, Pas HH, Yancey KB, Jonkman MF. Anti-epiligrin cicatricial pemphigoid and epidermolysis bullosa acquisita: differentiation by use of indirect immunofluorescence microscopy. J Am Acad Dermatol 2003;48(4):542–7.

[4] Parker SR, MacKelfresh J. Autoimmune blistering diseases in the elderly. Clin Dermatol 2011;29(1):69–79.

[5] Ishii N, Yoshida M, Hisamatsu Y, Ishida-Yamamoto A, Nakane H, Iizuka H, et al. Epidermolysis bullosa acquisita sera react with distinct epitopes on the NC1 and NC2 domains of type VII collagen: study using immunoblotting of domain-specific recombinant proteins and postembedding immunoelectron microscopy. Br J Dermatol 2004;150(5):843–51.

[6] Ishii N, Yoshida M, Ishida-Yamamoto A, Fritsch A, Elfert S, Bruckner-Tuderman L, et al. Some epidermolysis bullosa acquisita sera react with epitopes within the triple-helical collagenous domain as indicated by immunoelectron microscopy. Br J Dermatol 2009;160(5):1090–3.

[7] Bystryn JC, Akman A, Jiao D. Limitations in enzyme-linked immunosorbent assays for antibodies against desmogleins 1 and 3 in patients with pemphigus. Arch Dermatol 2002;138(9):1252–3.

[8] Cheng SW, Kobayashi M, Kinoshita-Kuroda K, Tanikawa A, Amagai M, Nishikawa T. Monitoring disease activity in pemphigus with enzyme-linked immunosorbent assay using recombinant desmogleins 1 and 3. Br J Dermatol 2002; 147(2):261–5.

E. Eugene Bain[a], Raminder K. Grover[b],*, Richard W. Plunkett[b], Ernst H. Beutner[a,b]

[a]Department of Dermatology, School of Medicine and Biomedical Sciences, University at Buffalo, State University of New York, Buffalo, NY 14203, USA;

[b]Beutner Laboratories and the Department of Microbiology and Immunology, School of Medicine and Biomedical Sciences, University at Buffalo, State University of New York, Buffalo, NY 14214, USA

*Corresponding author at: 138 Farber Hall, Beutner Laboratories and the Departments of Microbiology and Immunology, School of Medicine and Biomedical Sciences, University at Buffalo, SUNY, Buffalo, NY 14215, USA. Tel.: +1 716 838 0549; fax: +1 716 838 0798
E-mail address: rgrover2@buffalo.edu (R.K. Grover)

27 July 2011

Letter to the Editor

CYP4F22 is highly expressed at the site and timing of onset of keratinization during skin development

Autosomal recessive congenital ichthyoses (ARCI) include several subtypes: harlequin ichthyosis (HI), lamellar ichthyosis (LI) and congenital ichthyosiform erythroderma (CIE). To date, six causative genes have been identified in ARCI patients: *ABCA12, TGM1, NIPAL4, CYP4F22, ALOXE3* and *ALOX12B* [1]. The localization of transglutaminase 1, ABCA12 and 12R-lipoxygenase have been analyzed using samples from patients and model mice [1]. However, as for NIPAL4, CYP4F22, and lipoxygenase-3, neither localization nor function has been fully clarified yet. Herein, we investigate the expression pattern and localization of NIPAL4, CYP4F22 and lipoxygenase-3 in developing human epidermis and primary cultured normal human keratinocytes.

By quantitative reverse transcription (RT)-PCR analysis, at 10 and 14 weeks EGA, mRNA of *NIPAL4, CYP4F22* and *ALOXE3* was hardly expressed (Fig. 1A). The *CYP4F22* mRNA expression at 18
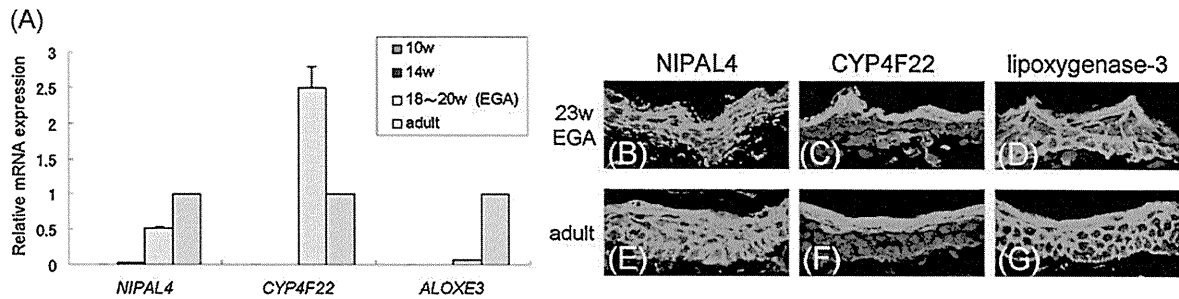
Fig. 1. NIPAL4, CYP4F22 and lipoxygenase-3 expression in developing human skin. (A) mRNA expression in developing human skin. The mRNA expression of *NIPAL4*, *CYP4F22* and *ALOXE3* in fetal human whole skin was studied by quantitative RT-PCR analysis, normalized by *GAPDH* [Applied Biosystems: Hs00398027_m1*, Hs00403446_m1*, Hs00222134_m1*, Hs03929097_ gl*]. At 10 and 14 weeks EGA, *NIPAL4*, *CYP4F22* and *ALOXE3* mRNA are hardly expressed. At 18–20 weeks EGA, the rate of *CYP4F22* mRNA expression is higher than in adult human whole skin (n = 3, mean ± SD). (B–G) Immunofluorescence staining of NIPAL4, CYP4F22 and lipoxygenase-3 in developing human skin. Fetal skin samples at 10–23 weeks EGA and adult skin samples were stained for NIPAL4 [Rabbit polyclonal anti-NIPAL4 antibody against a 16-amino acid sequence synthetic peptide (residues 445–461)], CYP4F22 [B01; Abnova, Taipei City, Taiwan], and lipoxygenase-3 [T-14; Santa Cruz Biotechnology, Santa Cruz, CA, U.S.A.] (Supplementary Fig. S1). For the 23 weeks EGA sample and the adult skin, CYP4F22 (C and F) is expressed in the upper layer of the epidermis, mainly in the granular layers. NIPAL4 (B and E) and lipoxygenase-3 (D and G) are expressed at the cell periphery throughout the epidermis. NIPAL4 expression is seen evenly from the basal cell layer to the granular layers, although lipoxygenase-3 expression is slightly stronger towards the granular layers. NIPAL4, CYP4F22 and lipoxygenase-3 green (FITC), nuclear stain, red (PI solution) (original magnification 40×). Data are presented as representative of triplicate experiments.

and 20 weeks EGA was higher than that in adult human skin. At 18 and 20 weeks EGA, *NIPAL4* mRNA expression was approximately half of that in adult skin, and only a tiny amount of *ALOXE3* mRNA was expressed.

We investigated protein localization by immunofluorescence staining (Fig. 1B–G). For the 10 weeks EGA sample, NIPAL4, CYP4F22 and lipoxygenase-3 were not detected. A similar pattern was obtained for the 14 weeks EGA sample. For the 23 weeks EGA sample, CYP4F22 was expressed in the upper layer of epidermis, mainly in the granular layers, and NIPAL4 and lipoxygenase-3 were expressed at the cell periphery in the entire epidermis. Staining patterns of NIPAL4, CYP4F22 and lipoxygenase-3 in the adult skin were similar to those at 23 weeks EGA. Lipoxygenase-3 is usually considered to be a partner with 12R-LOX. 12R-LOX has been visualized at the cell periphery only in the upper epidermis [2]. In our results, lipoxygenase-3 was distributed at the cell periphery in the entire epidermis. Concerning to lipoxygenase-3 in the upper epidermis, lipoxygenase-3 is thought to work with 12R-LOX, although function of lipoxygenase-3 in the lower epidermis is unknown.

In cultured keratinocytes, RT-PCR analysis (Fig. 2A) and immunoblot analysis (Fig. 2B and C) confirmed that mRNA and protein expression of CYP4F22 were increased under the high Ca^{2+} condition (1.2 mmol/L for 48 h). In contrast, there was no

significant increase in the mRNA or protein expression of NIPAL4 or ALOXE3 under the high Ca^{2+} condition.

The present study of the adult human epidermis clarified that NIPAL4 and lipoxygenase-3 were expressed at the cell periphery in the entire epidermis of adult human skin. CYP4F22 was expressed in the cytoplasm of keratinocytes in the upper layer of adult human epidermis, mainly in the granular layers. One previous report [3] noted that, inconsistent with our present observations, *NIPAL4* mRNA is highly expressed in the granular layers of the epidermis with *in situ* hybridization analysis. The cause of this discrepancy is unclear, but it might be due to difference in sensitivity between *in situ* hybridization and immunostaining.

We have demonstrated that the mRNAs of *NIPAL4*, *CYP4F22* and *ALOXE3* are not expressed in the early stages of fetal development, at 10 weeks EGA or at 14 weeks EGA. At 18 and 20 weeks EGA, *NIPAL4* mRNA expression was about half that in adult skin, although *ALOXE3* mRNA was only weakly expressed. Among the keratinization-associated genes, the mRNA expression pattern of *NIPAL4* is similar to that of *ABCA12*, and the pattern of *ALOXE3* resembles those of other keratinization-related molecules, such as *TGM1*, *LOR* and *KLK7* [4].

NIPAL4 encodes a putative transmembrane protein of 404 amino acids with a molecular weight of 44 kDa [6]. The NIPAL4 protein is highly expressed in the brain, lung and stomach, and in
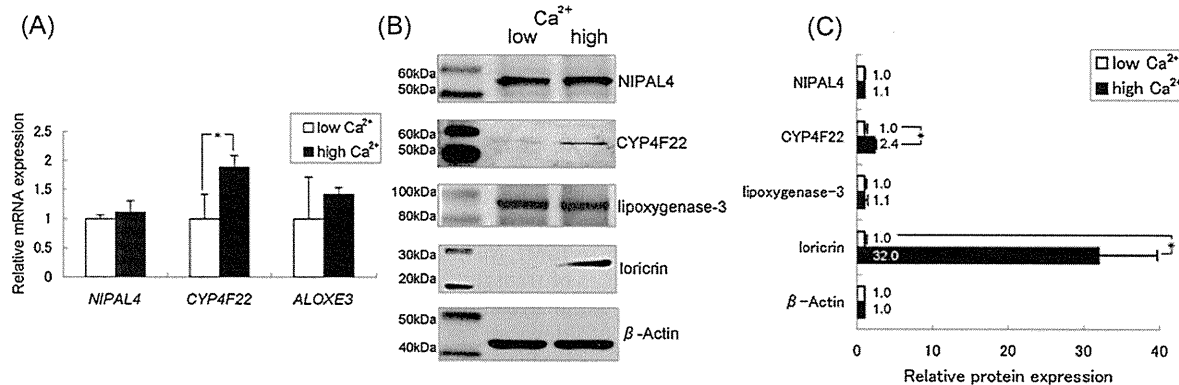

Fig. 2. mRNA and protein expression of NIPAL4, CYP4F22 and ALOXE3 in developing human skin and NHEK. (A) mRNA expression in NHEK. mRNA expression of *CYP4F22* is significantly higher in the NHEK under the high Ca^{2+} condition than in those under the low Ca^{2+} condition. There are no significant differences between the high and low Ca^{2+} conditions in terms of the mRNA expression of *NIPAL4* and *ALOXE3* (n = 3, mean ± SD, *p < 0.05). (B) Protein expression assessed by Western blot analysis. The expression of CYP4F22 is higher in the NHEK raised under the high Ca^{2+} condition than in those raised under the low Ca^{2+} condition. However, neither NIPAL4 nor lipoxygenase-3 is increased under high Ca^{2+} condition. Anti-ALOXE3 antibody for immunoblotting: NBP1-32533; Novus Biologicals, LLC, U.S.A. (C) Quantitative analysis by Image J software revealed that the protein expression of CYP4F22 was significantly increased under the high Ca^{2+} condition. Data are presented as representative of triplicate experiments.

leukocytes and keratinocytes. The protein product of the *ALOXE3* gene, lipoxygenase-3, is thought to function as a hydroperoxide isomerase to generate epoxy alcohol [5]. CYP4F22 is a member of the cytochrome P450 family 4, subfamily F. The gene includes 12 coding exons and the cDNA spans 2.6 kb in length. All *CYP4F22* mutations reported to date are predicted to abolish the function of the encoded CYP protein and to compromise the 12(R)-lipoxygenase (hepoxilin) pathway.

Human epidermis contains 15S-lipoxygenase type 1, 12S-lipoxygenase and 12R-lipoxygenase [6]. Skin also contains cytochrome 450, and members of the CYP4 family with unknown epidermal function [3]. 12R-lipoxygenase has attracted great medical interest. 12R-lipoxygenase is expressed only in the epidermis and the tonsils [6,7] and is upregulated in psoriatic lesions [8]. It transforms 20:4n-6 to 12R-hydroperoxyeicosatetraenoic acid (12R-HPETE), which is important for the development of the water permeability barrier function in the epidermis [2]. 12R-LOX and eLOX3 play a crucial role in releasing ω-hydroxyceramide for construction of the corneocyte lipid envelope which is essential for intact skin barrier [9]. O-linoleoyl-ω-hydroxyceramide is oxygenated by the consecutive actions of 12R-LOX and eLOX3 and the products are covalently attached to protein *via* the free ω-hydroxyl of the ceramide, forming the corneocyte lipid envelope [9].

It is hypothesized that CYP4F22 may be linked to the 12R-lipoxygenase and lipoxygenase-3 pathway. Hydroxyeicosatetraenoic acids (HEETs) can be hydrolyzed to triols by epoxide hydrolases, and these products might be substrates of CYP4F members. Thus, it is possible that CYP4F22 might be involved in a downstream step in the 12R-lipoxygenase/lipoxygenase-3 pathway. CYP4F22 could be involved in the oxidation of 8R,11R,12R-HEET. However, from a systemic study of MS/MS spectra of HEETs derived from 12- and 15-HPETE, CYP4F22 did not appear to oxidize 8R,11R,12R-HEET [10]. Nilsson et al. [10] reported that recombinant CYP4F22 catalyzed the omega-3 hydroxylation of 20:4n-6; however, oxygenation of 8R,11R,12R-HEET was not detected. An additional function of CYP4F22 is to synthesize the omega-hydroxy fatty acids in the ceramide [10].

Our study revealed CYP4F22 to be highly expressed at the site and the onset of keratinization during skin development. From this it is speculated that CYP4F22 is involved in the metabolism of lipid substrates that are important to differentiation/keratinization of epidermal keratinocytes, at least during the fetal period. Further studies of the function of CYP4F22 would be needed to elucidate its function in development of the epidermis and keratinocytes.

Acknowledgments

Appendix A. Supplementary data

Supplementary data associated with this article can be found, in the online version, at doi:10.1016/j.jdermsci.2011.12.006.

References

[1] Akiyama M. Updated molecular genetics and pathogenesis of ichthyoses. Nagoya J Med Sci 2011;73:79–90.
[2] Epp N, Fürstenberger G, Müller K, de Juanes S, Leitges M, Hausser I, et al. 12R-lipoxygenase deficiency disrupts epidermal barrier function. J Cell Biol 2007;177:173–82.
[3] Wajid M, Kurban M, Shimomura Y, Christiano AM. NIPAL4/ichthyin is expressed in the granular layer of human epidermis and mutated in two Pakistani families with autosomal recessive ichthyosis. Dermatology 2010;220:8–14.
[4] Yamanaka Y, Akiyama M, Sugiyama-Nakagiri Y, Sakai K, Goto M, McMillan JR, et al. Expression of keratinocyte lipid transporter ABCA12 in developing and reconstituted human epidermis. Am J Pathol 2007;171: 43–52.
[5] Eckl KM, Krieg P, Küster W, Traupe H, André F, Wittstruck N, et al. Mutation spectrum and functional analysis of epidermis-type lipoxygenases in patients with autosomal recessive congenital ichthyosis. Hum Mutat 2005;26:351–61.
[6] Holtzman MJ, Turk J, Pentland A. A regiospecific monooxygenase with novel stereopreference is the major pathway for arachidonic acid oxygenation in isolated epidermal cells. J Clin Invest 1989;84:1446–53.
[7] Boeglin WE, Kim RB, Brash AR. A 12R-lipoxygenase in human skin: mechanistic evidence, molecular cloning, and expression. Proc Natl Acad Sci USA 1998;95:6744–9.
[8] Woollard PM. Stereochemical difference between 12-hydroxy-5,8,10,14-eicosatetraenoic acid in platelets and psoriatic lesions. Biochem Biophys Res Commun 1986;136:169–76.
[9] Zheng Y, Yin H, Boeglin WE, Elias PM, Crumrine D, Beier DR, et al. Lipoxygenases mediate the effect of essential fatty acid in skin barrier formation. A proposed role in releasing omega-hydroxyceramide for construction of the corneocyte lipid envelope. J Biol Chem 2011;286:24046–5.
[10] Nilsson T, Ivanov IV, Oliw EH. LC–MS/MS analysis of epoxyalcohols and epoxides of arachidonic acid and their oxygenation by recombinant CYP4F8 and CYP4F22. Arch Biochem Biophys 2010;494:64–71.

Kaori Sasaki[a], Masashi Akiyama[a,b,*], Teruki Yanagi[a], Kaori Sakai[a], Yuki Miyamura[a], Megumi Sato[a], Hiroshi Shimizu[a]

[a]*Department of Dermatology, Hokkaido University Graduate School of Medicine, Sapporo, Japan;*
[b]*Department of Dermatology, Nagoya University Graduate School of Medicine, Nagoya, Japan*

*Corresponding author at: Department of Dermatology, Nagoya University Graduate School of Medicine, 65 Tsurumai-cho, Showa-ku, Nagoya 466-8550, Japan.
Tel.: +81 52 744 2314
E-mail address:* makiyama@med.nagoya-u.ac.jp (M. Akiyama)

1 August 2011

Correspondence

Possible modifier effects of keratin 17 gene mutation on keratitis–ichthyosis–deafness syndrome

MADAM, Keratitis–ichthyosis–deafness (KID) syndrome (OMIM 148210, 242150) is a rare type of ectodermal dysplasia caused by mutations in the gap junction protein beta-2 gene (GJB2)[1] or beta-6 gene (GJB6).[2] On the other hand, mutations in genes encoding keratin 6a, 6b, 16 and 17 (KRT6A, KRT6B, KRT16 and KRT17) are known to cause pachyonychia congenita (PC; OMIM 16720, 17210). PC and KID syndrome share similar symptoms, such as palmoplantar hyperkeratosis and onychodystrophy. This study reports a Japanese patient with atypical KID syndrome with the combined heterozygous mutations of a recurrent mutation in GJB2 and a novel mutation in the V1 region of KRT17.

The proband was a 40-year-old Japanese woman. She was the child of healthy, nonconsanguineous parents. From childhood, she had shown diffuse mutilating palmoplantar hyperkeratosis (Fig. 1a), nail dystrophy (Fig. 1b), hypotrichosis, sensorineural hearing loss, and vascularized keratitis. Periorificial hyperkeratosis was not seen. From these findings, the diagnosis of KID syndrome was made. She had had recurrent bacterial and fungal skin infections. In her twenties, painful tumours appeared on her lower limbs. In her thirties, tumours on both buttocks developed to take on a papilloma-like appearance (Fig. 1c). Etretinate with topical or systemic antibiotics and antifungal agents did not alleviate her symptoms. Skin abrasion was repeatedly conducted on the tumours. Histopathology of the lesions revealed epidermal pseudocarcinomatous hyperplasia with dilation of vessels in papillary and reticular dermis accompanied by mixed immune cell infiltrates, excluding the involvement of squamous cell carcinoma (Fig. 1d). Vacuolated keratinocytes, suggesting human papillomavirus infection, were not detected.

Genomic DNA extracted from peripheral blood was used as a template for polymerase chain reaction (PCR) amplification. Direct sequencing of GJB2, GJB6, KRT6A, KRT6B, KRT16 and KRT17 was performed as described elsewhere.[3–5] The medical ethical committee of Hokkaido University approved all the described studies. The study was conducted according to the Declaration of Helsinki Principles. The proband gave her written informed consent.

Mutation analysis of the proband's genomic DNA revealed a c.148G>A transition (p.Asp50Asn) in GJB2 (Fig. 2a), which is the most prevalent mutation in patients with KID syndrome.[1] Furthermore, the proband was found to be heterozygous for a c.177C>A transversion (p.Ser59Arg) in KRT17 (Fig. 2b). Restriction enzyme digestion of the PCR products by PvuII was carried out to confirm the c.177C>A in KRT17 (Fig. 2c). The c.177C>A in KRT17 was novel and was not detected in 200 alleles from 100 normal Japanese individuals. Mutation screening on the proband's parents could not be performed because the father was not alive and the mother did not consent. Keratin 17 (K17) immunohistochemistry on skin samples from several different sites revealed K17 expression in whole epidermis although its expression level did not vary between nonlesional and lesional skin specimens (data not shown).

As the clinical manifestations of the proband were atypical and more severe than those of other patients with KID syndrome – as evidenced, for example, by diffuse mutilating palmoplantar hyperkeratosis and recurrent granulation tissue formation on the buttock – we hypothesized that mutations in other genes might have affected the proband's phenotype through modifier effects. Modifier genes are defined as genes that affect the phenotypic expression of another gene, and several studies have demonstrated that modifier genes are involved in manifestations of inherited disorders.[6] KRT6A, KRT6B, KRT16 and KRT17, the causative genes of PC, which affects the nails and the palmoplantar area, were selected as candidates for modifier gene investigation in our case, although we cannot exclude the possibility that there are some other genes which modify KID syndrome phenotype.

Most of the keratin mutations are within the helix boundary motifs, which are crucial for keratin monomers to form dimers and subsequent keratin networks.[7] The KRT17 mutation found in the proband was located not within the helix boundary motifs but in the V1 region of K17 (Fig. 2d). In other keratin genes, such as KRT5 and KRT16, some mutations have been reported within the V1 region, and the phenotypes resulting from these mutations are milder than those resulting from the mutations within the helix boundary motifs.[7] The V1 regions of keratin intermediate filament have glycine loops[8] and it has been suggested that these structures modulate flexibility and other unknown physical attributes of keratin filaments by interacting with similar structures in loricrin.[9] Ser[59] is located within a highly conserved segment composed of the glycine loop in K17 (Fig. 2e). p.Ser59Arg in K17 is predicted to be probably damaging by PolyPhen-2, with a score of 0·893.[10]

Based on these findings, it is conceivable that the p.Ser59-Arg variant in K17 has a modifying effect on the pathogenic
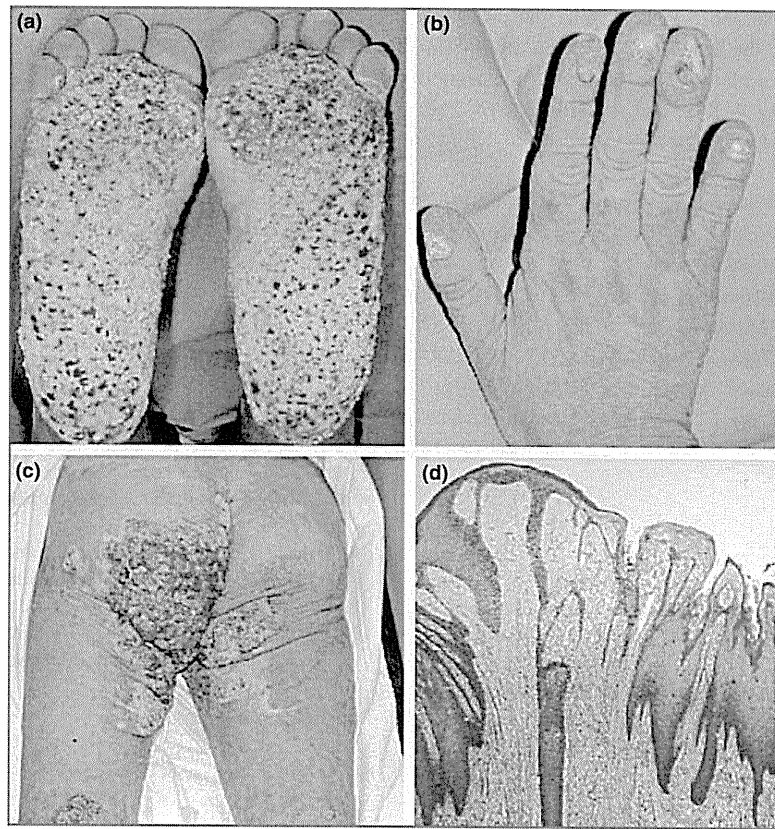
1

Fig 1. Clinical features of the proband. (a) Numerous erosive papules are coalesced into a hyperkeratotic plaque on the proband's soles. (b) Nail dystrophy is seen in the fingers. (c) A tumour is observed on the left buttock. Scars after skin abrasion are seen on the dorsal aspects of the thigh and on the right buttock. (d) Specimens from the tumour show pseudocarcinomatous hyperplasia of the epidermis. Dilated vessels with monocytic infiltrates are seen in the dermis (haematoxylin and eosin; original magnification × 100).
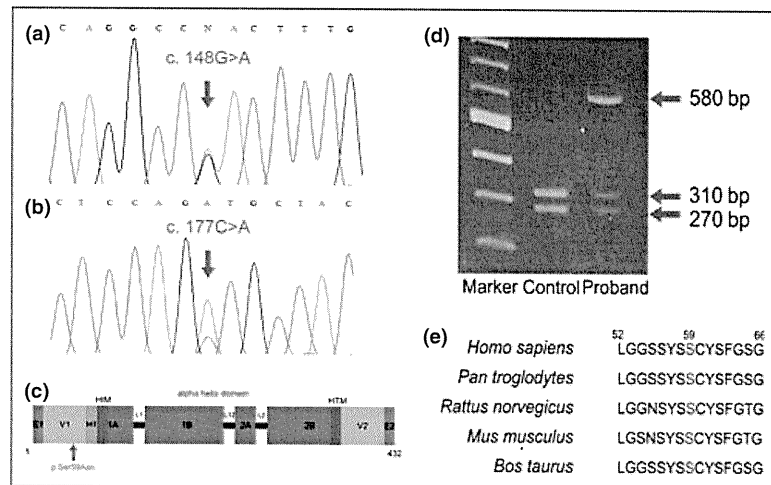

Fig 2. Mutation analysis. (a) The proband was heterozygous for a c.148G>A transition (p.Asp50Asn) mutation in GJB2 (arrow). (b) c.177C>A (p.Ser59Arg) in KRT17 was detected in the proband's genomic DNA (arrow). (c) PvuII restriction enzyme digestion of the polymerase chain reaction (PCR) products from genomic DNA of the proband and a normal control. c.177C>A resulted in the loss of a site for PvuII. PvuII restriction enzyme digestion of the PCR products from a normal controls reveals 270- and 310-bp bands. In contrast, 270-, 310- and 580-bp bands were detected in the proband, suggesting that she was heterozygous for c.177C>A. (d) A schematic of the structure of keratin 17. Note that Ser[59] is located at the V1 region of the keratin molecule (arrow). HIM, helix initiation motif; HTM, helix termination motif. (e) Keratin 17 amino acid sequence alignment shows the level of conservation in diverse species of the amino acid Ser59 (red characters).

GJB2 mutation p.Asp50Asn and may contribute the proband's phenotype. Nevertheless, the limited scope of this study (single case report) does not allow us to determine the clinical significance of p.Ser59Arg in K17, and the influence of other genetic and epigenetic factors cannot be excluded.

Department of Dermatology, Hokkaido   K. NATSUGA
University Graduate School of Medicine,   S. SHINKUMA*
North 15 West 7, Sapporo 060-8638, Japan   M. KANDA*
†Department of Dermatology, University of   Y. SUZUKI*
Miyazaki Faculty of Medicine, Miyazaki, Japan   N. CHOSA†
‡Department of Dermatology, Nagoya University   Y. NARITA†
Graduate School of Medicine, Nagoya, Japan   M. SETOYAMA†
E-mail: natsuga@med.hokudai.ac.jp   W. NISHIE*
    M. AKIYAMA*‡
    H. SHIMIZU*

References

1 Mazereeuw-Hautier J, Bitoun E, Chevrant-Breton J et al. Keratitis–ichthyosis–deafness syndrome: disease expression and spectrum of connexin 26 (GJB2) mutations in 14 patients. Br J Dermatol 2007; **156**:1015–19.

2 Jan AY, Amin S, Ratajczak P et al. Genetic heterogeneity of KID syndrome: identification of a Cx30 gene (GJB6) mutation in a patient with KID syndrome and congenital atrichia. J Invest Dermatol 2004; **122**:1108–13.

3 Richard G, White TW, Smith LE et al. Functional defects of Cx26 resulting from a heterozygous missense mutation in a family with dominant deaf-mutism and palmoplantar keratoderma. Hum Genet 1998; **103**:393–9.

4 del Castillo I, Villamar M, Moreno-Pelayo MA et al. A deletion involving the connexin 30 gene in nonsyndromic hearing impairment. N Engl J Med 2002; **346**:243–9.

5 Kanda M, Natsuga K, Nishie W et al. Morphological and genetic analysis of steatocystoma multiplex in an Asian family with pachyonychia congenita type 2 harbouring a KRT17 missense mutation. Br J Dermatol 2009; **160**:465–8.

6 Nadeau JH. Modifier genes in mice and humans. Nat Rev Genet 2001; **2**:165–74.

7 Szeverenyi I, Cassidy AJ, Chung CW et al. The Human Intermediate Filament Database: comprehensive information on a gene family involved in many human diseases. Hum Mutat 2008; **29**:351–60.

8 Steinert PM, Mack JW, Korge BP et al. Glycine loops in proteins: their occurrence in certain intermediate filament chains, loricrins and single-stranded RNA binding proteins. Int J Biol Macromol 1991; **13**:130–9.

9 Terrinoni A, Puddu P, Didona B et al. A mutation in the V1 domain of K16 is responsible for unilateral palmoplantar verrucous nevus. J Invest Dermatol 2000; **114**:1136–40.

10 Adzhubei IA, Schmidt S, Peshkin L et al. A method and server for predicting damaging missense mutations. Nat Methods 2010; **7**:248–9.